R-02-29

Groundwater flow simulations in support of the Local Scale Hydrogeological Description developed within the Laxemar Methodology Test Project

Sven Follin
SF GeoLogic AB

Urban Svensson
Computer-aided Fluid Engineering AB

May 2002

Svensk Kärnbränslehantering AB
Swedish Nuclear Fuel
and Waste Management Co
Box 5864
SE-102 40 Stockholm Sweden
Tel 08-459 84 00
+46 8 459 84 00
Fax 08-661 57 19
+46 8 661 57 19

ISSN 1402-3091
SKB Rapport R-02-29

Groundwater flow simulations in support of the Local Scale Hydrogeological Description developed within the Laxemar Methodology Test Project

Sven Follin
SF GeoLogic AB

Urban Svensson
Computer-aided Fluid Engineering AB

May 2002

Preface

An important part of the Swedish Nuclear Fuel and Waste Management Company (SKB) preparation for the site investigations starting in 2002 concerns Site Descriptive Modelling. SKB has conducted two parallel subprojects in this area. The first entailed establishing the first version (version 0) of the Site Descriptive Model of the three sites North Tierp, Forsmark and Simpevarp. An essential part of this work is compiling existing data and interpretations of these sites in a regional scale. The other subproject, concerns testing the Methodology for Site Descriptive Modelling by applying it to the existing data obtained from investigation of the Laxemar area, which is a part of the Simpevarp site. The latter subproject is primarily a methodology test. The lessons learned will be implemented in the Site Descriptive Modelling during the coming site investigation.

This report concerns a subproject that has been run in support of the methodology test project. The deduced Site Descriptive Model of the Laxemar area has been parameterised from a hydraulic point of view and subsequently put into practice in terms of a numerical flow model. The experiences made during this process and the outcome of the simulations have been presented to the methodology test project group in course of the project.

The intention of the subproject has been to explore the adaptation of a numerical flow model to site-specific surface and borehole data, and to identify potential needs for development and improvement in the planned modelling methodology and tools.

The work has been conducted in close co-operation with the methodology test project group, which consisted of representatives from the main disciplines, geology, hydrogeology, hydrogeochemistry and rock mechanics. The different experts assessed and evaluated data and explored different modelling options. However, the full project group also met at regular intervals to discuss on a detailed level the current progress and ideas of the different group members. In this way, the methodology test project also serves as a test bench for working interdisciplinary in order to reach a consistent understanding of a site.

Summary

The deduced Site Descriptive Model of the Laxemar area /Andersson et al, 2002/ has been parameterised from a hydraulic point of view and subsequently put into practice in terms of a numerical flow model. The intention of the subproject has been to explore the adaptation of a numerical flow model to site-specific surface and borehole data, and to identify potential needs for development and improvement in the planned modelling methodology and tools. The experiences made during this process and the outcome of the simulations have been presented to the methodology test project group in course of the project. The discussion and conclusions made in this particular report concern two issues mainly, (*i*) the use of numerical simulations as a means of gaining creditability, e.g. discrimination between alternative geological models, and (*ii*) calibration and conditioning of probabilistic (Monte Carlo) realisations.

Contents

1 Introduction

The Swedish Nuclear Fuel and Waste Management Company (SKB) is preparing for the site investigations scheduled to start in 2002. An important part of these preparations is to test the methodology for site descriptive modelling. SKB wants to demonstrate that a Site Descriptive Model can be established for a real site following structured and discipline integrated procedures in accordance with the intentions presented in the general execution programme /SKB, 2001/.

1.1 Background

As one of several means of preparation, a special project has been conducted, where the existing data from the Laxemar area, which is a part of the Simpevarp site, have been evaluated and interpreted into a Site Descriptive Model covering geology, hydrogeology, hydrogeochemistry and rock mechanics /Andersson et al, 2002/. The project is primarily a methodology test, but the lessons learned will be implemented in the pending modelling when new site-specific data become available.

This report concerns a subproject that has been run in support of the methodology test project. The deduced Site Descriptive Model of the Laxemar area has been parameterised from a hydraulic point of view and subsequently put into practice in terms of a numerical flow model. The experiences made during this process and the outcome of the simulations have been presented to the methodology test project in course of the project.

1.2 Scope of work

The intention of this project has been to explore the adaptation of a numerical flow model to site-specific surface and borehole data, and to identify potential needs for development and improvement in the planned modelling methodology and tools. Of particular interest in this work have been (*i*) to explore the usefulness of a method utilised by /Svensson, 2001/ for overall hydraulic parameter (transmissivity) calibration of unconditional fracture network realisations, (*ii*) discuss methods for local hydraulic parameter (transmissivity) calibration in order to match measured head responses, and (*iii*) using hydraulic modelling for assessing confidence in the descriptive model alternatives..

1.2.1 Objectives

The work has been conducted in order to reach the following objectives:

- construct a numerical flow model on a local scale, corresponding to version 1.2[1], for the Laxemar area /cf. SKB, 2001/,

[1] Version 1.2 of the Site Descriptive Model is a product of completed initial site investigations.

- through numerical simulations test (as well as contribute to) the evaluation and integration of site specific information with the planned methodology,
- through numerical simulations increase the understanding of the Laxemar area and, if possible, demonstrate how a creditability of the numerical flow model can be achieved/increased, and
- document experiences and uncertainties as well as suggest potential developments of current modelling methodology.

Hence, the present project has primarily been concerned with testing. The numerical flow model that has been constructed in support of the methodology test project should be reasonable, but it can not be regarded as a "real" version 1.2 as there are limitations both in input data and in the scope of the analysis, see Section 1.2.2.

1.2.2 Limitations in scope

The construction of a numerical flow model was a priori confined by the methodology test project to treat version 1.2 of the Laxemar area solely. Consequently, there was limited consideration taken to the postulated format of the general execution programme /SKB, 2001/, which suggests two model versions previous to version 1.2, namely a version 0 and a version 1.1. This limitation is essentially motivated by the fact that the methodology test project has primarily been concerned with testing the evaluation and integration of detailed site specific information on a local scale (cf. the footnote on the previous page). It should be noted, however, that the postulated version 0 regional Site Descriptive Model of the Simpevarp site has been developed in another project that was run in parallel to the methodology test project.

Although regional modelling was not performed, available regional knowledge was of course used also for the methodology test project and the site descriptive modelling of the Laxemar area. For example, the results from the regional numerical flow modelling conducted by /Svensson, 1997a/ has been used as a means to evaluate the implications of the chosen location and extent of the *Laxemar model area* as well as the chosen boundary conditions used for the local numerical flow modelling.

The locations of the Laxemar model area and the regional model area studied by /Svensson, 1997a/ are shown in Figure 1-1. The latter was used as a regional model area for Aberg in SKB's safety assessment project SR 97 /SKB, 1999/. In addition, Figure 1-1 shows the locations of the Simpevarp regional model area and the local model area for Aberg. The topographic relief along the surface profile is shown below the map. The relief implies a regional topographic gradient of c. 3–4‰, which is more or less equivalent to the maximum super regional topographic gradient between the peak of the southern Swedish Highlands and the Baltic Sea.

The intermediate version of the DarcyTools software package available at the time of the project did not have full compatibility with all intended functions from a site descriptive modelling point of view. In particular, the numerical simulations carried out in this project have been constrained to treat steady-state flow solely. It should be noted, however, that the current version (1.0) of DarcyTools /Svensson et al, 2002/ is not subjected to this limitation[2].

[2] The numerical simulation of the coming Site Descriptive Models will be carried out with, at least, version 2.0 of DarcyTools and version 7.1 of NAMMU.

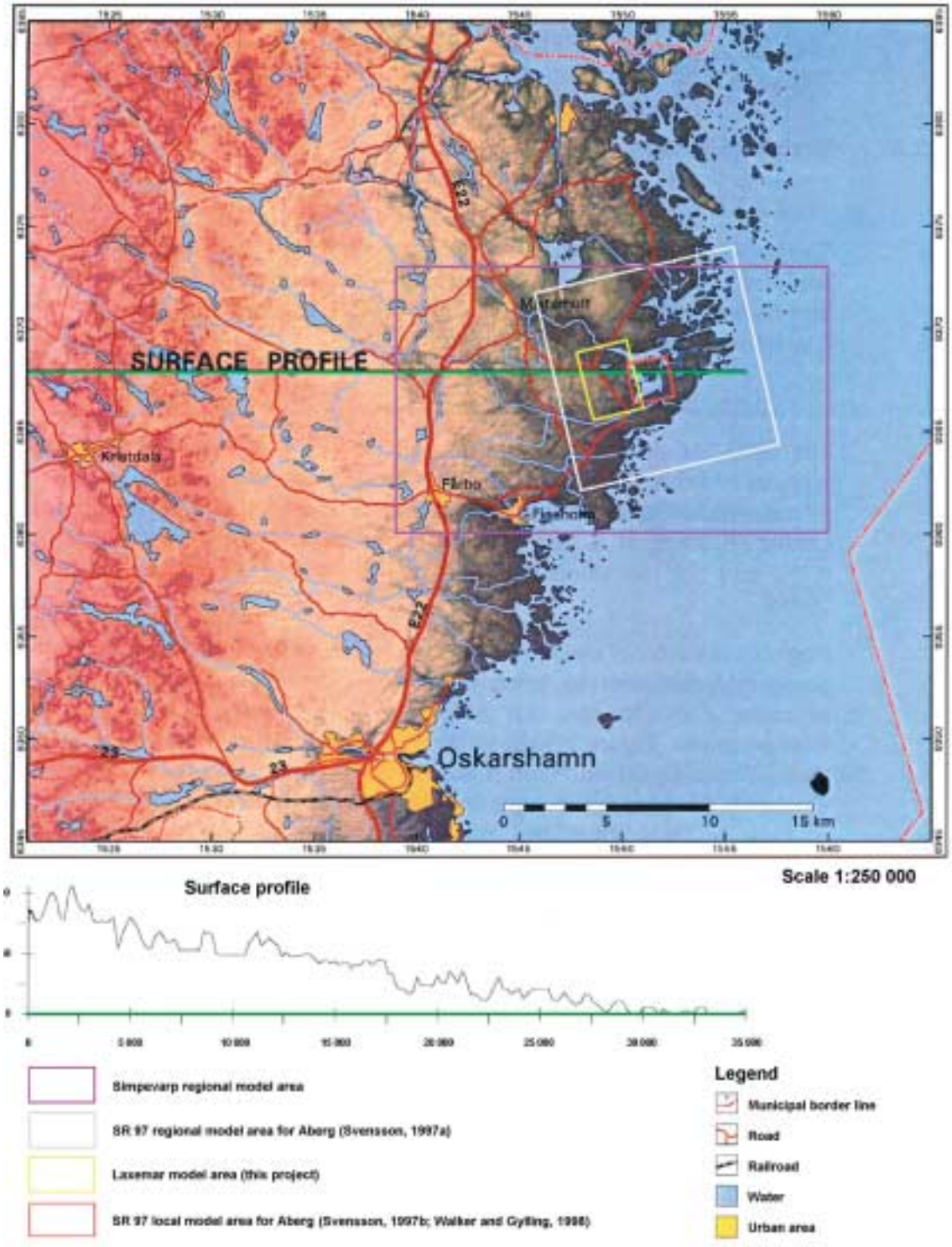

Figure 1-1. *Locations of the Laxemar model area and the Simpevarp regional model area. The SR 97 regional and local model areas for Aberg are also shown. The topographic relief along the surface profile implies a regional topographic gradient of c. 3–4‰.*

Although the limitation to steady-state flow is essentially motivated by the fact that an intermediate version of the DarcyTools software package was used, it should be kept in mind that the regional numerical flow modelling conducted by /Svensson, 1997a/ also was carried out for steady-state flow. This fact does not imply that steady-state flow is a correct simplification but it relaxes the limitation of the numerical flow modelling carried out in this project.

In addition to the limitation listed above, the following components of the numerical flow model were omitted, or made with a moderate ambition level:

- There was no consideration taken to transport properties or processes other than those related to variable-density flow and the hydrodynamic dispersion of saline groundwater.
- Surface hydrology was included to the extent possible given the status of the current hydrological knowledge about the site.

These limitations are essentially motivated by the fact that the methodology test project has primarily been concerned with testing. Furthermore, some "method descriptions" for modelling and intermediate products of modelling were in a developing phase, thus unavailable during the conduct of the current project. As a matter of fact, the project has partly been a test bed for some of these method descriptions.

Finally, the version (2.3) of the RVS software package available at the time of the project did not have full compatibility with all intended functions as specified in the geometric-geological modelling report /Munier and Hermanson, 2001/. In particular, the used version of RVS was not able to store results of "property" modelling. This means that the description of the three-dimensional distribution of properties in different rock units had to be handled outside the RVS-environment. In concrete words, version 9.03 of the Tecplot software has been used for visualisation of input and output data to meet the hydrogeological needs of the project. It should be noted, however, that the development of the RVS software package is still ongoing and the current version (3.0) of RVS differs in many aspects from the previous one.

2 Mathematical modelling

2.1 General modelling approach

Figure 2-1 illustrates SKB's general modelling approach to hydrogeological modelling of groundwater flow through fractured crystalline rocks. The division into hydraulic domains (HSD, HRD and HCD) is described in Chapter 7 of the general execution program for site investigations /SKB, 2001/. The hydrogeological setting is described by means of parameters, which detail:

- the *geometric and hydraulic properties* of the Quaternary deposits (HSD) and the crystalline bedrock (HRD and HCD), and
- the *hydrological processes* that govern the hydraulic interplay between surface water and groundwater including groundwater flow at repository depth.

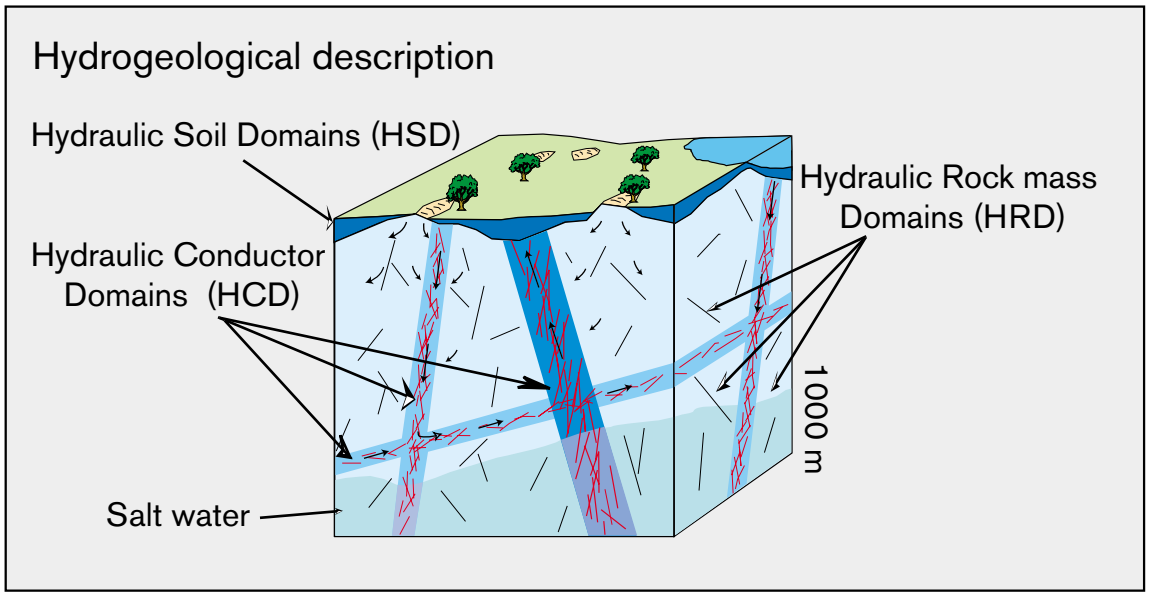

Figure 2-1. *The Quaternary deposits (soil) and the crystalline bedrock are divided into separate hydraulic domains denoted HSD, HRD and HCD. Within each domain the hydraulic properties are represented by mean values or by spatially distributed statistical distributions /SKB, 2001/.*

2.2 Code description

The geometric and hydraulic properties of the Quaternary deposits and the crystalline bedrock have been implemented into a numerical model using the software package DarcyTools. DarcyTools is a finite volume code for variable-density groundwater flow /Svensson et al, 2002/. DarcyTools uses a mixed DFN/continuum approach for the simulation of groundwater flow through fractured rocks, which means that the geometries and the transmissivities of all discrete features, deterministic as well as probabilistic, are transformed to equivalent inter-cell conductivities prior to the solution of the governing equations.

2.2.1 Governing equations

The governing equations of variable-density groundwater flow and transport in porous media may be written as:

Mass Conservation

The fluid mass balance equation is

$$\frac{\partial(\varepsilon\rho)}{\partial t} = -\nabla\cdot(\varepsilon\rho\mathbf{v}) + Q_p, \tag{1}$$

where $\varepsilon(x, y, z, t)$ is a dimensionless porosity, $\rho(x, y, z, t)$ is the fluid density, $\mathbf{v}(x, y, z, t)$ is the average fluid velocity, $Q_p(x, y, z, t)$ is the fluid mass source, x, y and z are spatial coordinates, t is time, and ∇ is the divergence operator. It is generally assumed that density is a linear function of concentration /see, e.g. Voss, 1984/:

$$\rho = \rho_0 + \frac{\partial\rho}{\partial C}(C - C_0) \tag{2}$$

where ρ_0 is the fluid density at a base concentration C_0 and $\partial\rho/\partial C$ is a constant coefficient of density variability.

With variable fluid density the fluid flow equation is expressed in terms of the pressure variable since the potential head function does not exist. The pressure gradient form of Darcy's law is

$$\mathbf{v} = -\left(\frac{\mathbf{k}}{\varepsilon\mu}\right)\cdot(\nabla p - \rho\mathbf{g}) \tag{3}$$

where $p(x, y, z, t)$ is the groundwater pressure, $\mathbf{g}$ is the gravity vector, μ is fluid dynamic viscosity, and $\mathbf{k}(x, y, z)$ is the intrinsic permeability tensor.

Salt Conservation

For a single species stored in solution (e.g. salt), the solute mass balance equation may be expressed as

$$\frac{\partial(\varepsilon \rho C)}{\partial t} = -\nabla \cdot (\varepsilon \rho \mathbf{v} C) + \nabla \cdot [\varepsilon \rho (D_0 \mathbf{I} + \mathbf{D}) \cdot \nabla C] Q_p C^* \quad (4)$$

where D_0 is the apparent molecular diffusivity in a porous medium of solutes in solution, **I** is the dimensionless identity tensor, and C^* is the concentration of fluid sources expressed as a mass fraction. /Bear, 1979/ has formulated the components of the mechanical dispersion tensor **D** to account for both transverse and longitudinal dispersivities.

As stated in Section 1.2.2, the intermediate version of the DarcyTools software package available at the time of the project did not have full compatibility with all intended functions from a site descriptive modelling point of view. In particular, the numerical simulations carried out in this project have been constrained to treat steady state flow and transport solely. It should be noted, however, that the current version (1.0) of DarcyTools /Svensson et al, 2002/ is not subjected to this limitation.

2.2.2 Representation of vectors and tensors

The representation of vector and tensor properties in DarcyTools is based on the control volume concept. For each grid cell in a 3D mesh, there are six directional control volumes. The computation of the associated cell wall properties is schematically illustrated in Figure 2-2, which treats three simple examples of the inter-cell conductivity between two adjacent pressure nodes in a 2D mesh.

For a discrete fracture network, the cell wall or inter-cell hydraulic conductivity is determined by the conductivity-weighted volume that the intersecting fractures make with the control volume, see Figure 2-2. The transmissivity T_f and thickness b_f of a fracture define its hydraulic conductivity K_f.

$$K_f = T_f / b_f \quad (5)$$

The geometric and hydraulic properties of the fractures are either deterministic or probabilistic. The geometric and hydraulic properties of the deterministic fractures are obtained from the Site Descriptive Modelling, which builds on an interdisciplinary interpretation of, e.g. *lineament maps*, *airborne and ground geophysics*, and various *borehole investigations and hydraulic measurements*.

The size of the probabilistic fractures are in the intermediate version of DarcyTools assumed to follow a power law distribution based on the findings of /La Pointe et al, 1999/. Given the power law exponent, D, and the volume, V, of the model domain, the number of fractures (squares), N, within a specified size range, L_1 to L_2, can be estimated using the following equation /Svensson, 2001/:

$$N[L_1, L_2] = \frac{V\ I}{D}\left[\left(\frac{L_2}{L_{ref}}\right)^D - \left(\frac{L_1}{L_{ref}}\right)^D\right] \quad (6)$$

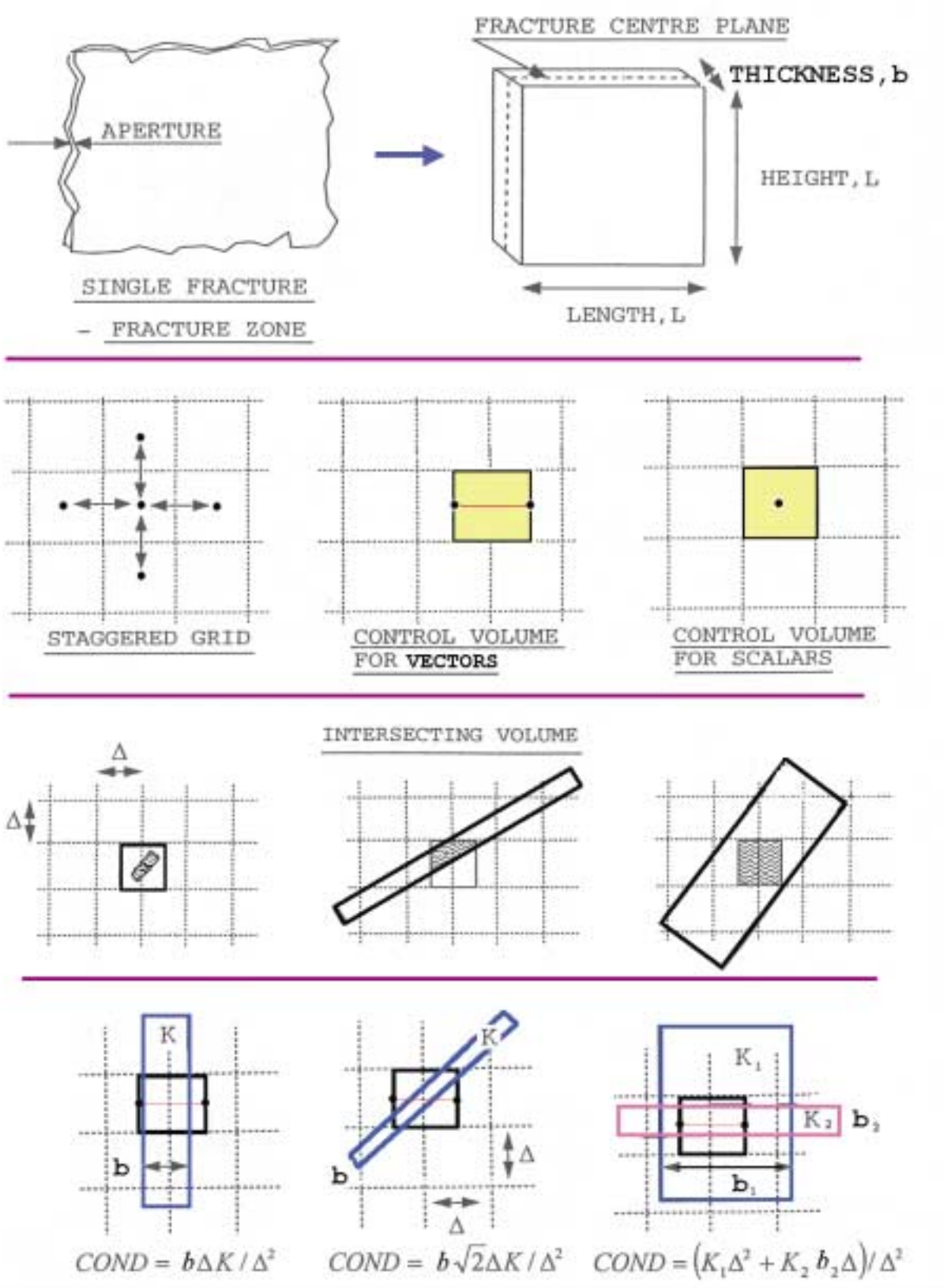

Figure 2-2. *Schematic view of the definition of inter-cell hydraulic conductivity (COND; •—•) in DarcyTools. Modified after /Svensson, 1999/.*

where $L_1 < L_2$. I and L_{ref} are two coefficients that determine the position of the power law distribution in a log-log plot of N versus L. For the structural-hydraulic model of the prototype repository at Äspö, /Svensson, 2001/ used $I = 10^{-8}$ and $L_{ref} = 500$ m with good results.

Besides fracture size, the key geometric parameters of a probabilistic fracture network are orientation, intensity (P_{32}) and spatial distribution. Input data for the assessment of these parameters come from the *trace mapping of outcrops and borehole core logs*.

The intermediate version of the DarcyTools software package available at the time of the project was programmed to treat the transmissivity T_f and thickness b_f of the probabilistic fractures as functions of the fracture size L_f.

$$T_f = \alpha \left(\frac{L_f}{100} \right)^2 \tag{7}$$

$$b_f = 0.01\, L_f \tag{8}$$

The coefficient α in Equation (7) was used to calibrate the overall transmissivity field of each unconditional fracture network realisation, see Chapters 3 and 4. In Chapter 3, an alternative approach based on DFN-analysis of single-hole packer test is discussed.

2.2.3 Representation of scalars

The derivation of scalar properties in DarcyTools is also based on the control volume concept, with one exception; the control volume for a scalar entity is node centred, see Figure 2-2. Variables such as pressure, salinity, porosity and saturation are all scalars.

The intermediate version of the DarcyTools software package available at the time of the project was programmed to treat the kinematic porosity n of a fracture as the ratio between the empirically based transmissivity-transport aperture e_T and the fracture thickness b_f defined in Equation (8).

$$e_T = 2T^{0.6} \tag{9}$$

$$n = \left(e_T / b_f \right) \tag{10}$$

Conclusively, the transport properties and the storage properties in DarcyTools are based on the assumption of a power law size distribution.

2.2.4 Surface runoff and groundwater recharge

Whenever the top boundary of the model domain coincides with ground surface, the net precipitation should be used as a flux boundary condition in order to allow for a correct treatment of the groundwater recharge process. Since the recharge rate is a part of the solution, a saturation algorithm is used to determine whether the top cell should be recharged or if surface runoff prevails. The majority of the recharged net precipitation is discharging in the nearest topographic low.

3 Sources of information and model set-up

The Laxemar area was included in the pre-investigations of the Äspö Hard Rock Laboratory during 1986–1990. These investigations comprised different surface based methods, some percussion-drilled boreholes and hydraulic testing of one deep (KLX01, 1 059 m) core-drilled borehole /Stanfors et al, 1997/. In 1992, a second deep (KLX02, 1 660 m) borehole was core-drilled mainly to test all sorts of investigation techniques at great depths including interference testing /see Ekman (ed.), 2001/. There were also additional percussion holes drilled. In conclusion, there are two deep core-drilled boreholes in the area and 12 rather shallow (~100 m) percussion-drilled boreholes. In order to incorporate all available information, it was decided by the methodology test project group to set the depth of the Laxemar model domain to 2 000 m.

The numerical model set-up presented in this study is based partly on hydrogeological investigations and partly on a 3D geological model provided by the different experts of the methodology test project group. The hydrogeological investigations comprise (*i*) meteorological and surface hydrological investigations, and (*ii*) borehole investigations, tests and monitoring. The 3D geological model comprise mapping (interpretations) of Quaternary deposits and bedrock geology (rock type, lineaments and deformation zones). The reader is kindly referred to Chapters 2 and 3 of the methodology test project report /Andersson et al, 2002/ for a detailed description of the gathered data about the Laxemar model area, as this would be an unnecessary duplication of efforts.

3.1 Overview

The Laxemar area constitutes the mainland immediately to the west alongside the Äspö island, see Figure 3-1. The area is situated within the nature geographic region "Södermanlands and Götalands archipelagos". The landscape is a mixture of open water areas, islands and skerries. The vegetation is characterised by relatively poor forest types, with pine as the dominating tree species, although spots of deciduous wood exist in the lower, sediment filled valleys. These sediments are mainly used as pasture.

The predominant rock type is a reddish grey, c. 1 800 Ma, medium- to coarse-grained porphyretic granite to granodiorite belonging to the Trans-Scandinavian Igneous Belt (TIB). Exposed bedrock or bedrock with a thin (<0.5 m) layer of Quaternary deposits, mostly till, dominate the area. Glacial and post-glacial sediments dominate in the topographic lows (valleys), see Figure 3-1.

The crystalline basement contains deformation zones on a large variety of scales ranging from micro-cracks in the 'intact rock', individual visible joints, to regional fault zones. The associated lineaments may be divided into two main groups, deterministic and non-deterministic. In SKB's nomenclature the deterministic lineaments are generally denoted 'local major zones' and 'regional zones' depending on their size. In conclusion, the remaining lineaments are in the modelling considered non-deterministic. It is important to note that the definition of deterministic and non-deterministic is not static but a matter of scale, resolution and available information.

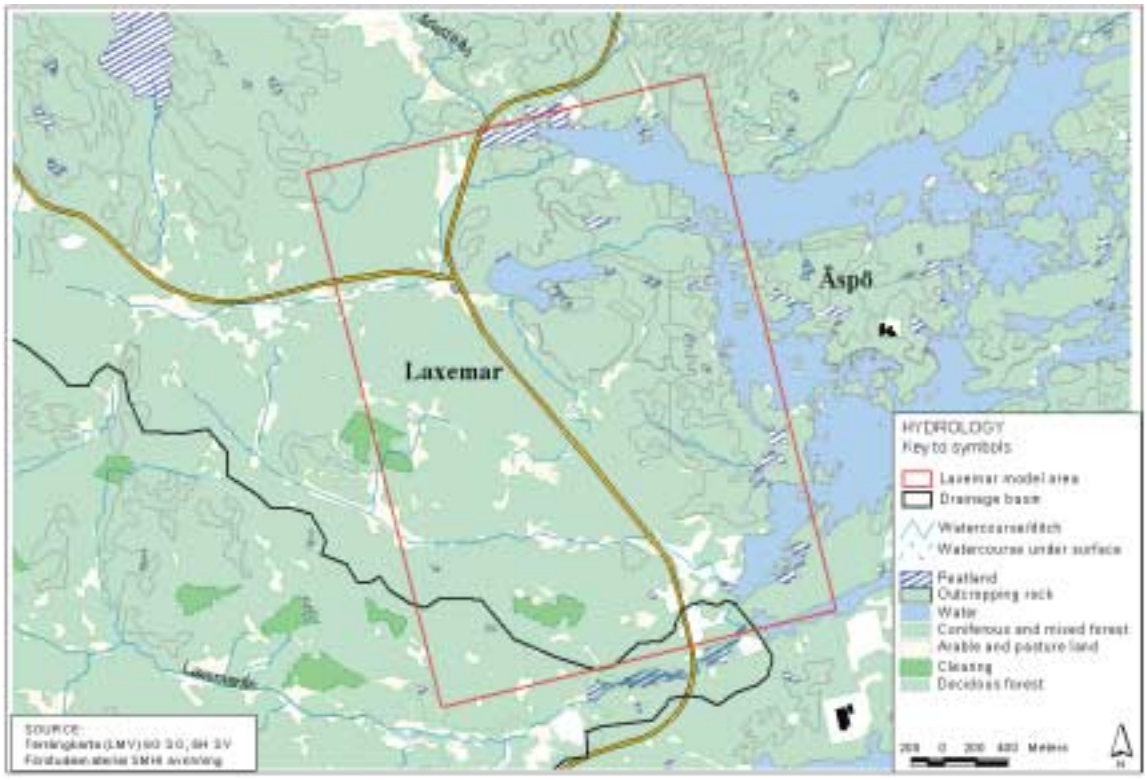

***Figure 3-1**. Plan view of the landscape in the proximity of the Laxemar area. Outcropping bedrock (contoured) or bedrock with a thin (<0.5 m) layer of Quaternary deposits (green), mostly till, dominate the area. Glacial and post-glacial sediments dominate in the topographic lows (yellow). The surface water body in the northern part is Lake Frisksjön.*

In the methodology test project, the main sources of information used for the identification (interpretation) of deterministic zones have been lineament maps, BIPS images of the core-drilled boreholes, borehole radar reflectors and ground surface seismic reflectors.

3.2 Base and Alternative geological model

Figure 3-2 shows a plan view of the lineaments in the Laxemar model area that have been interpreted as deterministic fracture zones by /Andersson et al, 2002/. Lineaments greater than 1 000 m are defined as local major or regional fracture zones.

Figure 3-3 shows isometric views of the Base and the Alternative geological model, respectively. Both models are discussed in the methodology test report. However, this study treats the Base geological model only. The main motive for this simplification was the constrained timetable of the project.

The Base geological model contains 21 lineaments longer than 1 000 m and the Alternative geological model contains 20. Thus, the major structural difference between the two "deterministic" models is not the number of fracture zones but the strike and dip of some of the zones, see Figure 3-3.

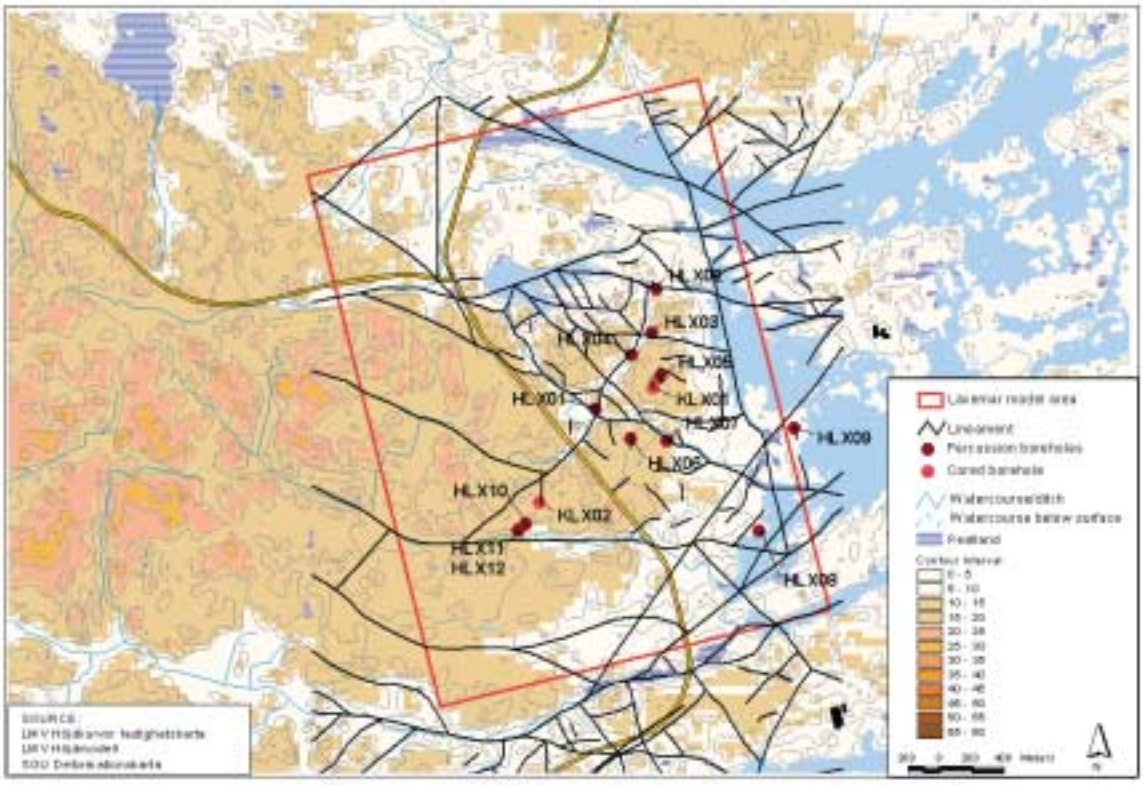

Figure 3-2. *Map showing the Base geological model of the Laxemar area with contour lines of the topography and locations of the core-drilled and percussion-drilled boreholes.*

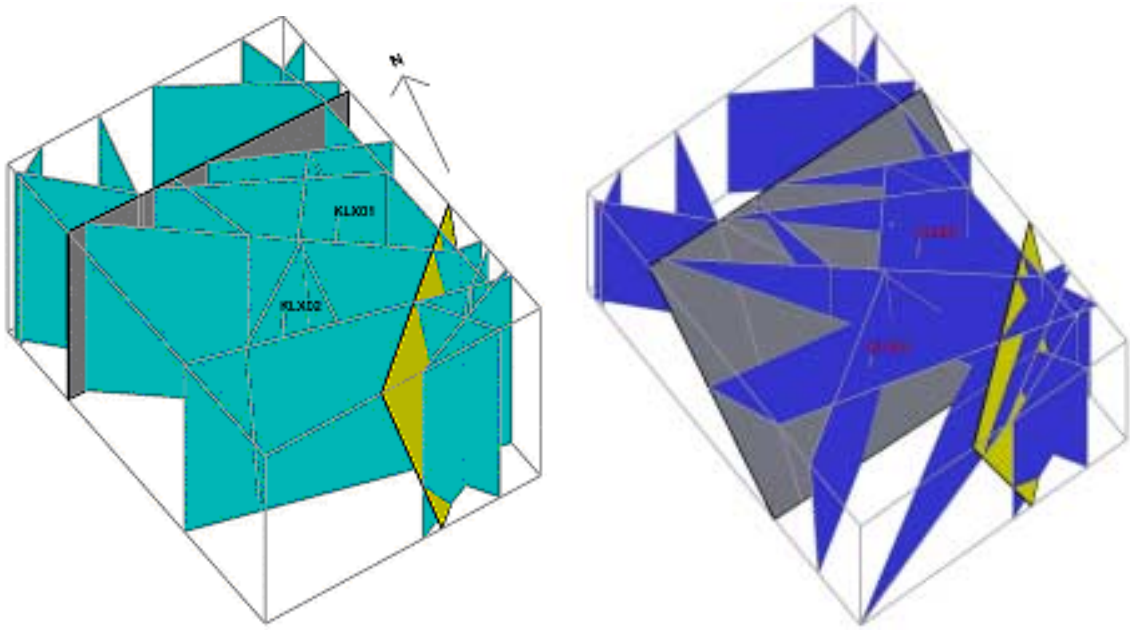

Figure 3-3. *Isometric views of the Base geological model (left) and the Alternative geological model (right). The different colours denote the size of the lineament, related to the zone; grey = regional; blue, turquoise = local, major and local; yellow = regional magnetic.*

The existing investigations and documentation of the *Quaternary deposits and bedrock geology* are reviewed and scrutinised in Sections 3.1–3.3 of the methodology test report. From a hydrogeological perspective, the interpretations presented in Sections 4.1 of the methodology test report constitute the basis for the *geometric modelling* of the different hydraulic domains in the Laxemar area. Thus, Sections 3.1–3.3 and 4.1 and the underlying references provide input to:

- The 3D geometry of the 21 deterministic fracture zones and lineaments (HCD) of the Base geological model, see Figure 3-4, and intervening rock volumes (HRD).
- The distribution of Quaternary deposits (HSD), including genesis, composition, thickness and depth (cf. Figure 3-1). In should be noted that the HSD has not been treated in detail in this study nor in the methodology test project.

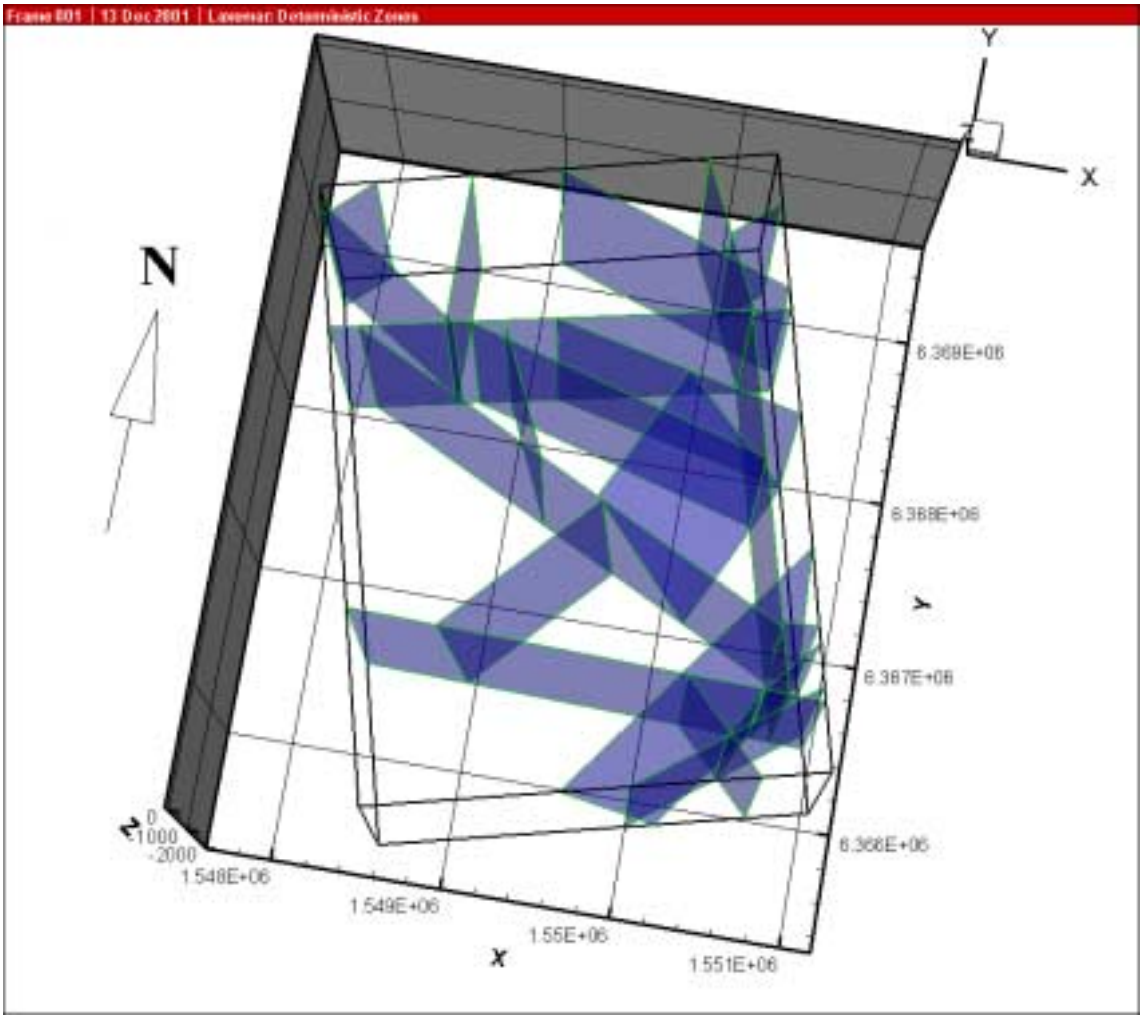

Figure 3-4. *Visualisation of the interpreted 3D geometry of the 21 deterministic fracture zones and lineaments (HCD) of the Base geological model. The dimensions of the model domain are Length × Width × Height = 3 400 × 2 500 × 2 000 m³, i.e. 17 km³.*

3.3 Meteorology and hydrology

The existing data from the investigations and documentation of the *meteorology and hydrology* are compiled in Section 3.6 of the methodology test report. From a hydrogeological perspective, the compilation in Section 3.6 and the shore level displacement described in Sections 3.1 and 3.9 constitute the basis for *hydrological process modelling* of the Laxemar area. In concrete words, the data compilations in Sections 3.1, 3.6 and 3.9 provide input to:

- The present-day interpretation of drainage areas, as well as mapping of springs, wetlands and streams, surveying of land use such as ditching and damming projects, water supply resources, nature conservation areas, etc, see Figure 3-5.
- Mean estimates of the precipitation and runoff. Heads and flows in the watercourses are also of interest, but unfortunately there are no such measurements carried out within the Laxemar model area.
- An assessment of the relative impact of local topography, shore level displacement and variable-density groundwater flow versus the role of inferred fracture zones for the definition of initial and boundary conditions and the numerical simulation of present-day and future recharge and discharge areas of groundwater flow.

The topography of the Laxemar area is slightly more accentuated compared to the conditions at Äspö and adjacent islands. The maximum altitude exceeds 22 m.a.s.l. in the western part and the maximum topographic gradient within the area is c. 30‰, see Figure 3-6, which is about one order of magnitude greater than the regional topographic gradient shown in Figure 1-1.

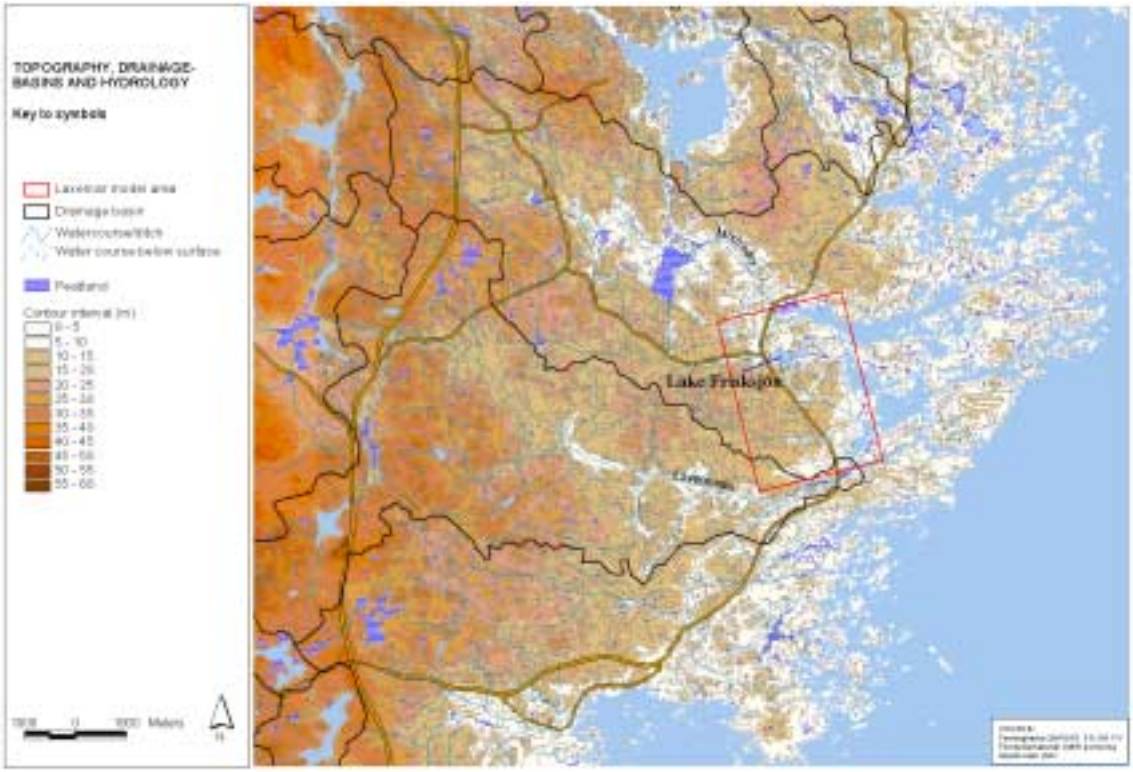

Figure 3-5*. The model area is located right in between the watercourses Laxermarån and Mistraån. The only major terrestrial surface water body within the model area is Lake Frisksjön.*

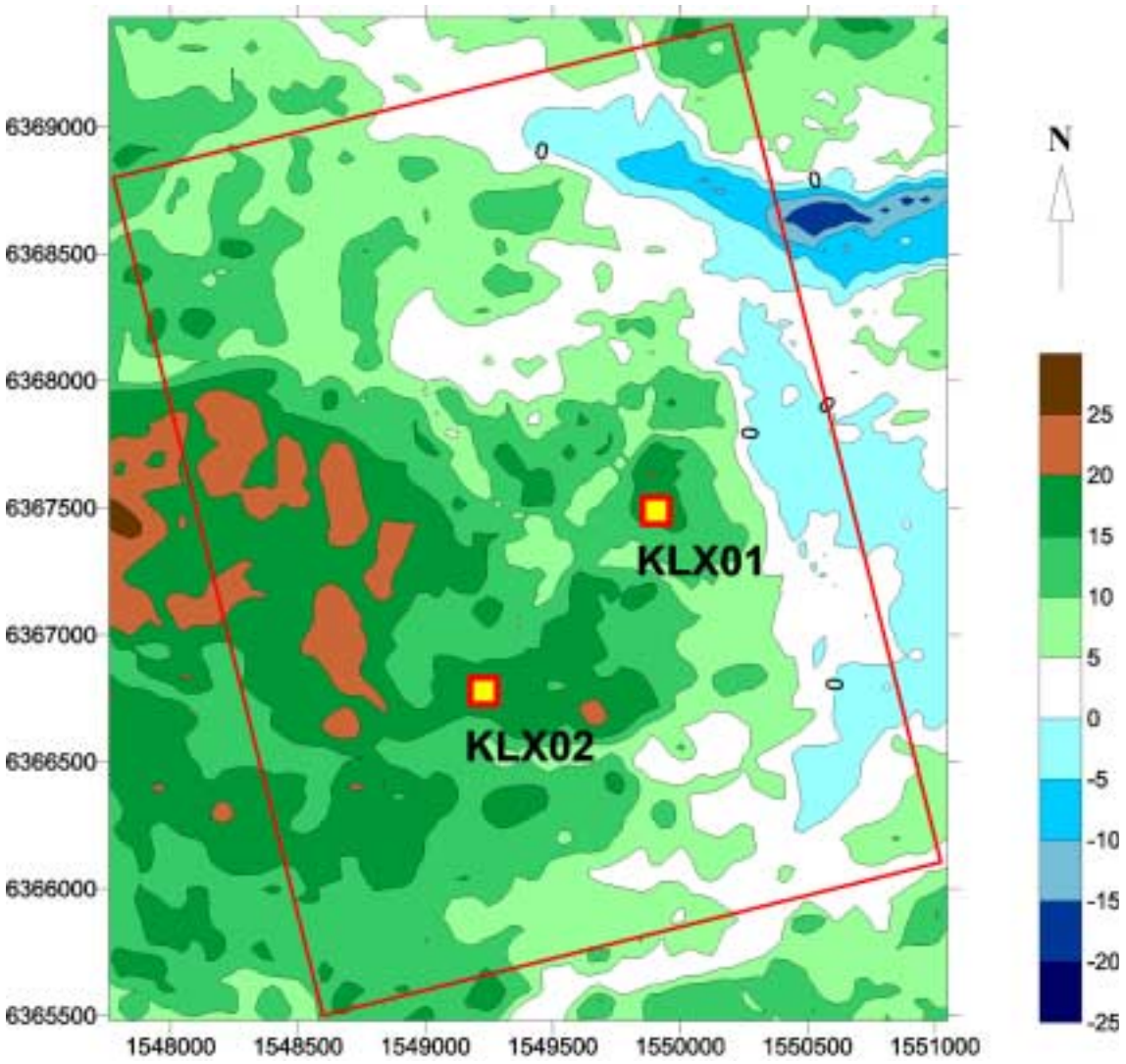

Figure 3-6. *The maximum altitude within the Laxemar model area (red border line) slightly exceeds 22 m.a.s.l. in the western part. The maximum topographic gradient within the area is c. 30‰. The locations of the two deep core-drilled boreholes KLX01 and KLX02 are shown as reference.*

According to the shore level displacement model presented by /Påsse, 1996, 1997/, the Laxemar area began to rise above the prevailing seal level c. 9 500 BP, see Figure 3-7. However, the area was subsequently subjected to a transgression between 9 000 and 7 000 BP. The Litorina Sea is the probably the most important aquatic stage for the present-day groundwater composition along the Swedish east coast. Between 5 200 BC–3 200 BC, the salinity in the Litorina Sea was as high as 12–15‰ (20‰) /Westman et al, 1999/. Since then, the salinity has decreased to the present-day salt concentration of the Baltic Sea, c. 7‰ (c. 6‰ in the proximity to Äspö due to out flowing freshwater). During this period, however, an increasing portion of the Laxemar model area was subjected to freshwater flushing starting at c. 6 000 BP. Since 2 000 BP the body of the model area has been above sea level. The present-day mean runoff has been estimated to c. 150–200 mm/year. Even if only a minor portion of the runoff recharges to the groundwater in the basement, it is likely that the freshwater flushing has reached a quasi steady state with the saline groundwater beneath.

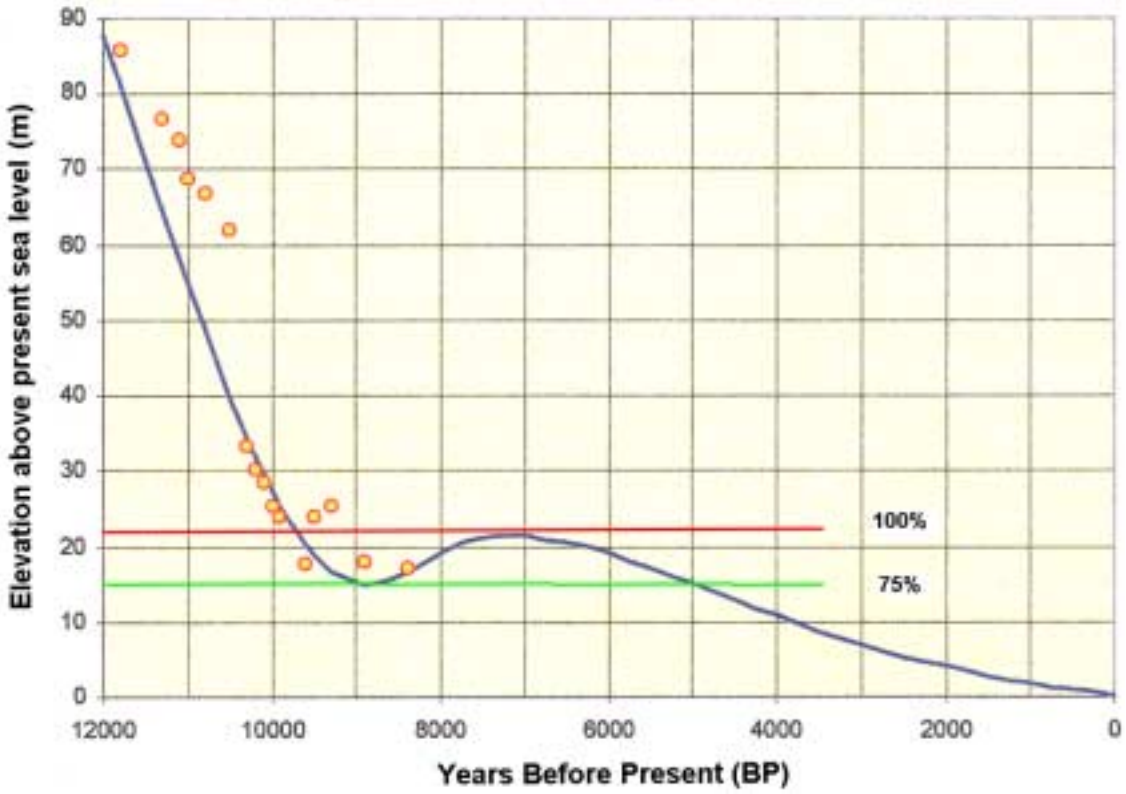

Figure 3-7. *Measured (circles) and modelled (graph) shore level displacement in southeast Sweden. The horizontal lines indicate the percentage of the Laxemar model area that was covered by seawater at 7 000 BP (red line) and at 5 000 BP (green line). (Modified after /Follin et al, 1998/.*

3.4 Borehole investigations and monitoring

The existing investigations and documentation of *borehole investigations and monitoring* are reviewed and compiled in Sections 3.7, 3.8 and 3.9 of the methodology test report. The decisions made for the definition *of geometric and hydraulic properties* of the different hydraulic domains are presented in Section 4.2 of the same report.

Based on the hydraulic testing of the two deep core-drilled boreholes KLX01 and KLX02 and their geometric intercepts with the inferred fracture zones, it was concluded by the methodology test project group to assign different hydraulic properties to the 21 deterministic fracture zones and lineaments shown in Figure 3-2. The deduced parameter values are compiled in Table 3-1 and visualised in Figure 3-8.

Table 3-1. Hydraulic properties of the 21 deterministic fracture zones and lineaments.

No. of fracture zones	Transmissivity (m^2/s)	Thickness (m)	Colour in Figure 3-8
2	1×10^{-4}	15	Red
2	7×10^{-6}	15	Yellow
17	3×10^{-6}	15	Blue

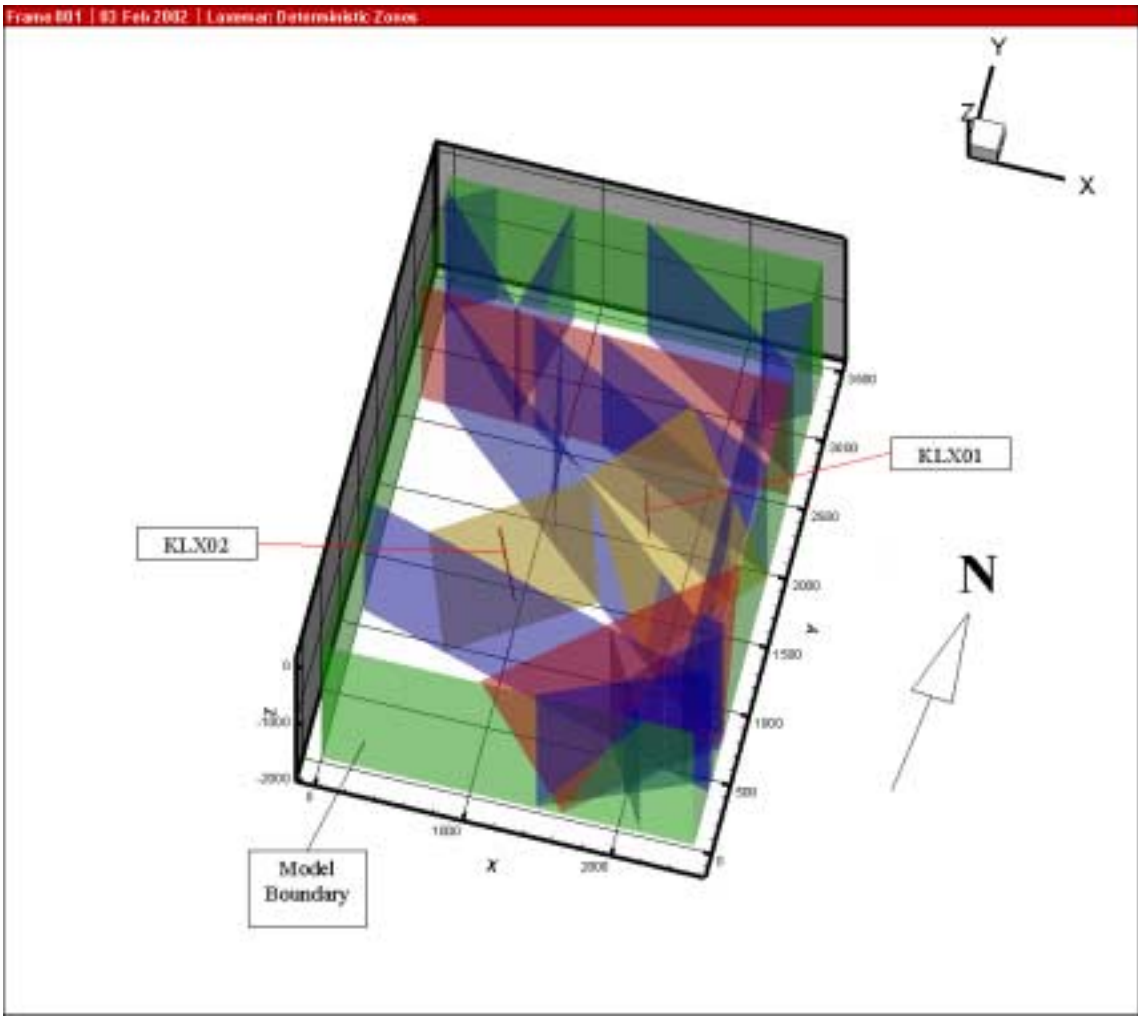

Figure 3-8. *3D visualisation of the Laxemar model domain. The vertical boundaries of the model domain are coloured in green. The strike direction of the model's y-axis is N14°W. Different hydraulic properties have been assigned to the 21 deterministic fracture zones and lineaments. The properties are compiled in Table 3-1.*

It is important to note that the interpretation methodology behind the structural model of the Laxemar area shown in Figures 3-2, 3-4 and 3-8 is based on available geological and geophysical data on the scale of the model area. The fracture zones and lineaments in these figures have not been derived as a result of mixing multiple sources of information on a variety of support scales. Hence, the interpreted fault traces are deterministic given the constraints and uncertainties of underlying sources of information described in Sections 3.1–3.3 and 4.1 of the methodology test report.

In spite of the trustworthiness of the used methodology, it is important to note that the relatively small number of short lineaments in figure 3-2 may be a scale effect /La Pointe et al, 1999/. The shortest lineament within the Laxemar model area deterministically described by the methodology test project group is c. one kilometre. Thus, the occurrence of fracture zones below this size may need to be treated stochastically depending on the problem formulation and the available knowledge.

According to the general execution programme /SKB, 2001/, a limited number of boreholes will be drilled during the site investigations. Hence, it is reasonable to expect that the geometric and hydraulic properties of the discrete features within the model domain will be treated deterministically above some threshold of size probabilistically below.

The DFN analyses carried out in preparation of Section 3.8 of the methodology test report provide a means for a probabilistic treatment of the geometric and hydraulic properties of all non-deterministic fractures and fracture zones. The underlying principle of probabilistic modelling is based on two fundamental assumptions; statistical homogeneity and ergodicity /see, e.g. de Marsily, 1986/. In concrete words, it may be advocated that the geometric and hydraulic properties of all non-deterministic fractures and fracture zones obey the same statistics as the studied field observations.

Based on the DFN analyses of available trace map data in Section 3.8 of the methodology test report, it was concluded by the methodology test project group to characterise the non-deterministic fracturing within the Laxemar model domain by means of four fracture sets. The deduced parameter values are compiled in Table 3-2.

The power law exponent for the fracture size, D, was not possible to assess with certainty in Section 3.8 due to a varying quality and censoring in the available trace map data. According to /La Pointe et al, 1999/, the value of the exponent given in Table 3-2 should be diagnostic for probabilistic 3D structural-hydrogeological simulations in the region where the Laxemar area is located. Given the value of the power law exponent and the volume, V, of the Laxemar model domain (cf. Figure 3-4), the number of fractures (squares), $N[L_1, L_2]$, within a specified size range, L_1 to L_2, can be estimated using the following equation (cf. Chapter 2):

$$N[L_1, L_2] = \frac{V\ I}{D}\left[\left(\frac{L_2}{L_{ref}}\right)^D - \left(\frac{L_1}{L_{ref}}\right)^D\right] \qquad (11)$$

where $L_1 < L_2$. I and L_{ref} are two coefficients that determine the position of the power law distribution in a log-log plot of N versus L. For the structural-hydraulic model of the prototype repository at Äspö, /Svensson, 2001/ used $I = 10^{-8}$ and $L_{ref} = 500$ m with good results.

Table 3-2. Geometric and hydraulic properties for the non-deterministic fractures.

Set	Orientation statistics of the mean normal vector (pole)				Fracture size	Spatial distribution	Fracture intensity*	
No.	Type	Trend	Plunge	Dispersion	D	Type	P_{32}	P_{32c}
1	Fisher	262.0	03.8	8.52	–2.6	Baecher	0.78	0.12
2	Fisher	195.9	13.7	9.26	–2.6	Baecher	0.66	0.15
3	Fisher	135.9	07.9	9.36	–2.6	Baecher	0.76	0.12
4	Fisher	035.4	71.4	7.02	–2.6	Baecher	0.24	0.08
All	** $T \in logN(4.2\times10^{-8}, 2\times10^{-7})$ m²/s				[$\equiv log_{10}T \in N(-8.06, 0.773)$]		2.44	0.48

*P_{32} = all P_{32c} = conductive
**$logN$ = lognormal distribution N = normal distribution

Figure 3-9 shows the result of applying Equation (1) with $D = -2.6$, $L_{ref} = 500$ m and $I = 10^{-8}$ to the Laxemar model domain. The graph shows that the number of fractures increases drastically as the fracture size decreases. For the purpose of this project it was decided by the authors to carry out the probabilistic modelling of non-deterministic fractures using a window of 30–800 m. As indicated in Figure 3-9, this window contains approximately 100 000–200 000 fractures. There are two main motives for using the adopted window, namely the discretisation of the flow model mesh and the size of the smallest deterministic fracture zone. As already mentioned in Chapter 2, the resolution of the model mesh was set to 30 m by the methodology test project group due to the length of straddle interval of the single-hole double-packer tests in the two deep core-drilled boreholes KLX01 and KLX02. Consequently, fractures less than 30 m of length are not treated geometrically in the structural-hydraulic flow model. Moreover, according to Figure 3-4, the smallest deterministic fracture zone is c. one kilometre.

The soundness of the graph in Figure 3-9 is an open question. However, according to the data compilation in Table 3-3, the chosen parameter values yield c. 20 fracture zones in the interval 800 m–3 200 m, a value that fits the number of deterministic zones concluded for the Laxemar area by the methodology test project group, see Figure 3-8.

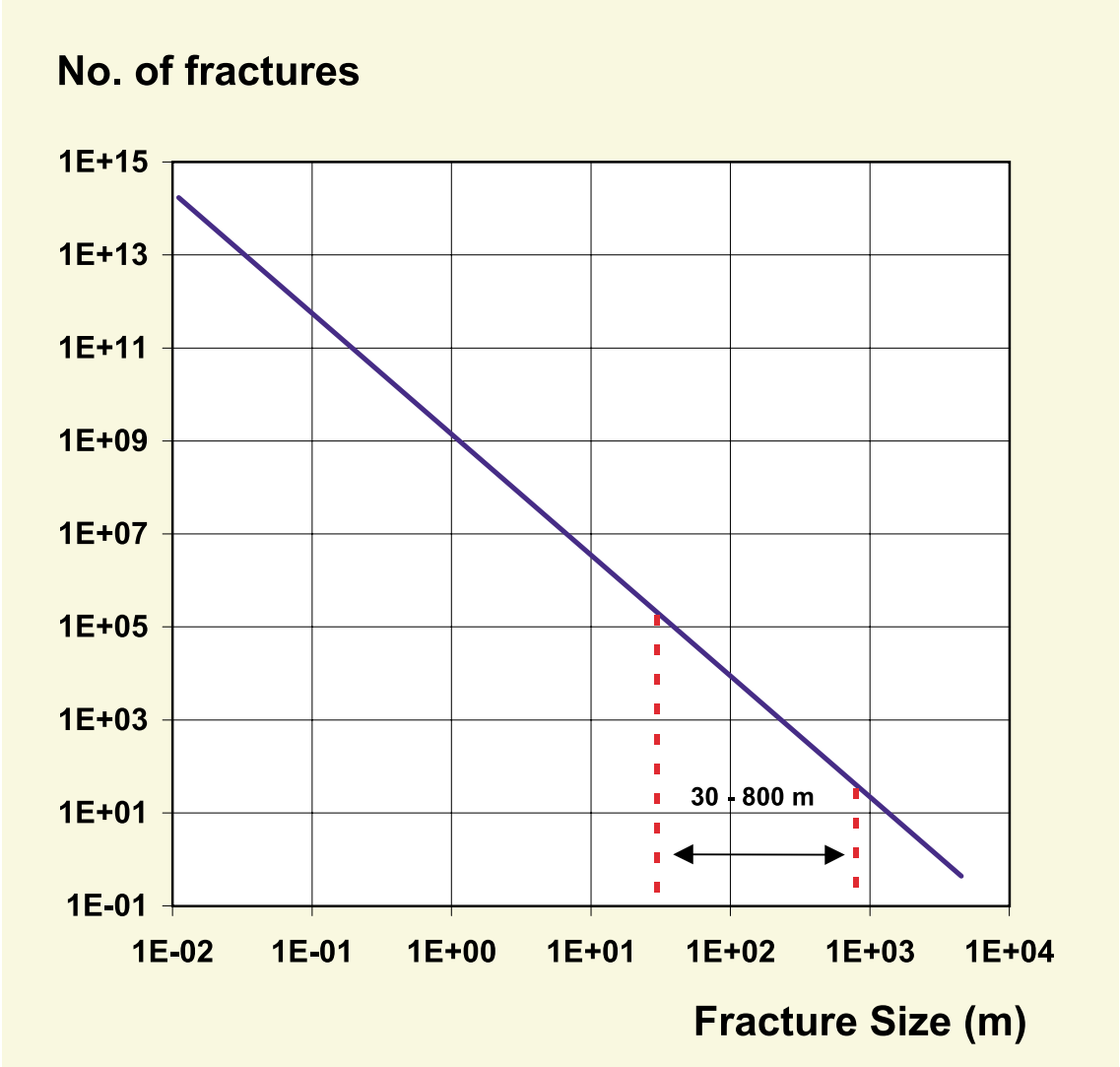

Figure 3-9. *Anticipated number of fractures in the Laxemar model domain as a function of fracture size. Application of Equation (1) with V =17 km³, D = –2.6, L_{ref} = 500 m and I = 10^{-8}.*

Table 3-3. Anticipated number of fractures in the Laxemar model domain as a function of fracture size. Application of Equation (1) with V = 17 km³, D = –2.6, L_{ref} = 500 m and I = 10^{-8}.

Upper limit L_2	Lower limit L_1	No. of fractures $N[L_2, L_1]$	Fracture intensity $P_{32}[L_2, L_1]$	$P_{32}[6\,400, L_1]$
6 400	3 200	1	4.14E–04	>4.14E–04
3 200	1 600	3	6.28E–04	1.04E–03
1 600	800	17	9.51E–04	1.99E–03
800	400	98	1.44E–03	3.44E–03
400	200	592	2.19E–03	5.62E–03
200	100	3586	3.31E–03	8.93E–03
100	50	21737	5.02E–03	1.40E–02
50	25	131787	7.61E–03	2.16E–02
25	12.5	799006	1.15E–02	3.31E–02
12.5	6.25	4844267	1.75E–02	5.06E–02
6.25	3.125	29370139	2.65E–02	7.71E–02
3.125	1.5625	1.78E+08	4.02E–02	1.17E–01
1.5625	0.78125	1.08E+09	6.09E–02	1.78E–01
0.78125	0.390625	6.55E+09	9.23E–02	2.70E–01
0.390625	0.195313	3.97E+10	1.40E–01	4.10E–01
0.195313	0.097656	2.41E+11	2.12E–01	6.22E–01
0.097656	0.048828	1.46E+12	3.21E–01	9.44E–01
0.048828	0.024414	8.84E+12	4.87E–01	1.43E+00
0.024414	0.012207	5.36E+13	7.38E–01	2.17E+00
0.012207	0.006104	3.25E+14	1.12E+00	3.29E+00

The next to the last column in Table 3-3 shows the calculated contribution of each fracture size interval to the fracture intensity and the last column shows the accumulated fracture intensity. If one compares the bottom line values for the accumulated fracture intensity in Table 3-3 with the reported P_{32} value in Table 3-2, it may be concluded that the body of the inferred fracture intensity in Section 3.8, is a consequence of a large number of small fractures. For the chosen discretisation of the Laxemar structural-hydraulic flow model (30 m), the P_{32} value is 0.023, see Figure 3-10.

The significance of a threshold in the fracture intensity depends on the problem formulation and the temporal and spatial scales involved. The effect of a large number of small fractures may be taken into account in a numerical flow model by adding a continuous field of low conductivities to a discrete field of high conductivities. This approach has been used in the present study. Concerning transport, however, the subgrid threshold is judged to be a quite complex artefact. A recent approach by /Svensson et al, 2002/.

The fracture transmissivity distribution of the DFN-analyses behind Table 3-2 is not correlated to the fracture size distribution. Both /Stigsson et al, 2000/ and /Svensson, 2001/ have developed detailed flow models of the bedrock in proximity to the Prototype repository at Äspö, but come to quite different conclusions regarding the impact of a correlation between transmissivity and size. The former authors conclude that a correlation between fracture transmissivity and fracture size yields unrealistic flow rates, a conclusion that is contradicted by the findings of the latter author.

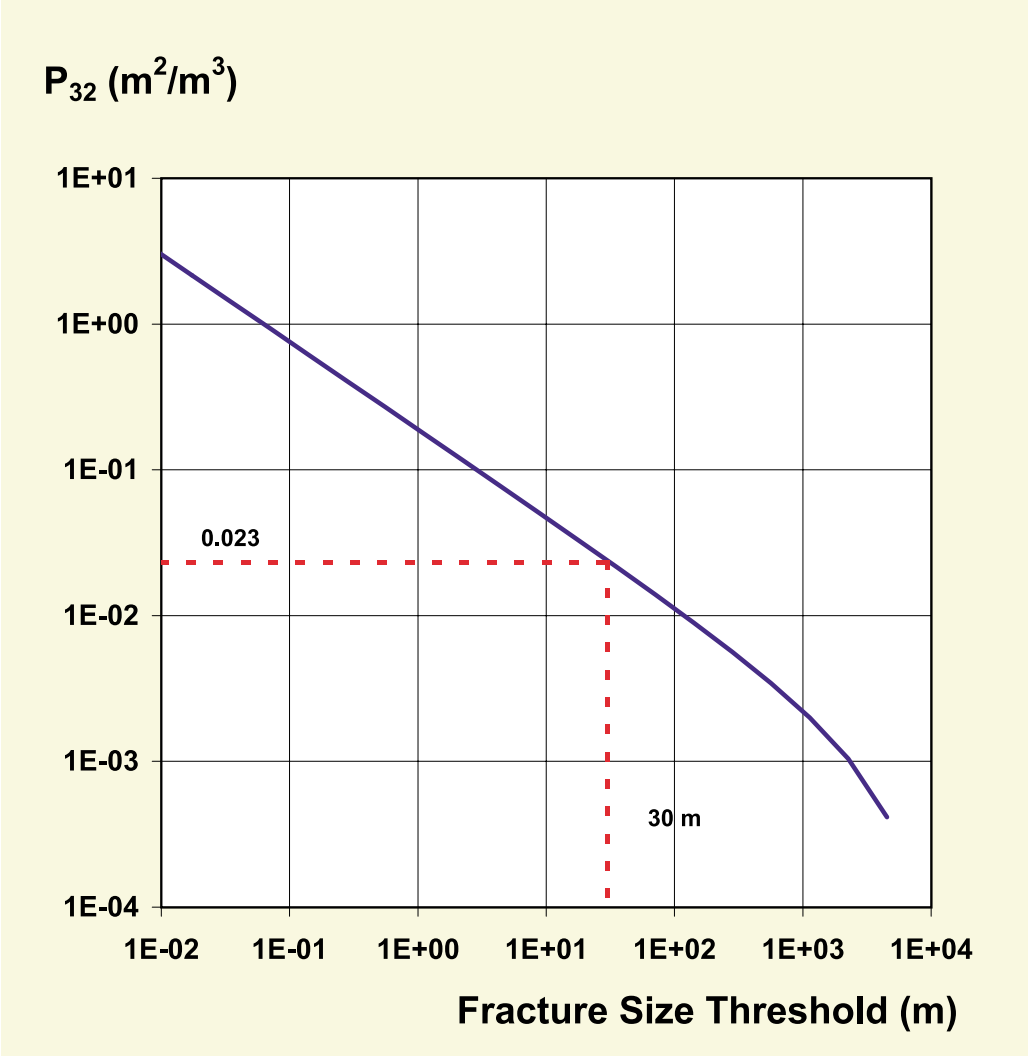

Figure 3-10. *P_{32} as a function of the fracture size threshold. For the used discretisation of the Laxemar structural-hydraulic flow model, 30 m, the P_{32} value is of the order of 0.02–0.03.*

Correlated or not, the correlation suggested by /Svensson, 2001/ has been adopted in the present study. The main motive for using the suggested relationships between (*i*) fracture transmissivity and size, and (*ii*) fracture thickness and size, see Equations (12) and (13), is the many observations of an underlying power law principle for fractured crystalline rock properties /Vicsek, 1989; Turcotte, 1992; Barton and La Pointe, 1995/.

$$T_f = \begin{cases} \alpha \left(\dfrac{L_f}{100} \right)^2 \text{m}^2/\text{s} & \text{for } L_f \le 100\,\text{m} \\ \alpha \quad \text{m}^2/\text{s} & \text{for } L_f > 100\,\text{m} \end{cases} \tag{12}$$

$$b_f = 0.01\, L_f \tag{13}$$

The value of the coefficient α in Equation (2a) was set to 10^{-5} m^2/s in the study by /Svensson, 2001/. By means of trial and error, this value was altered to 10^{-8} m^2/s in the present study in order to obtain a good fit with measured conductivities on a 30 m scale in the core-drilled boreholes KLX01 and KLX02. The result of the calibration process is displayed in Chapter 4. The plot in Figure 3-11 visualises the different proposals for the definition of fracture transmissivity discussed so far.

As previously mentioned, the impact of a subgrid threshold on the probabilistic fracture intensity has been taken into account in the present study by adding a continuous field of low conductivities to the discrete field of high conductivities. As pointed out by /Svensson, 2001/, a continuous field of low conductivities may be used as an extra tuning knob in the calibration.

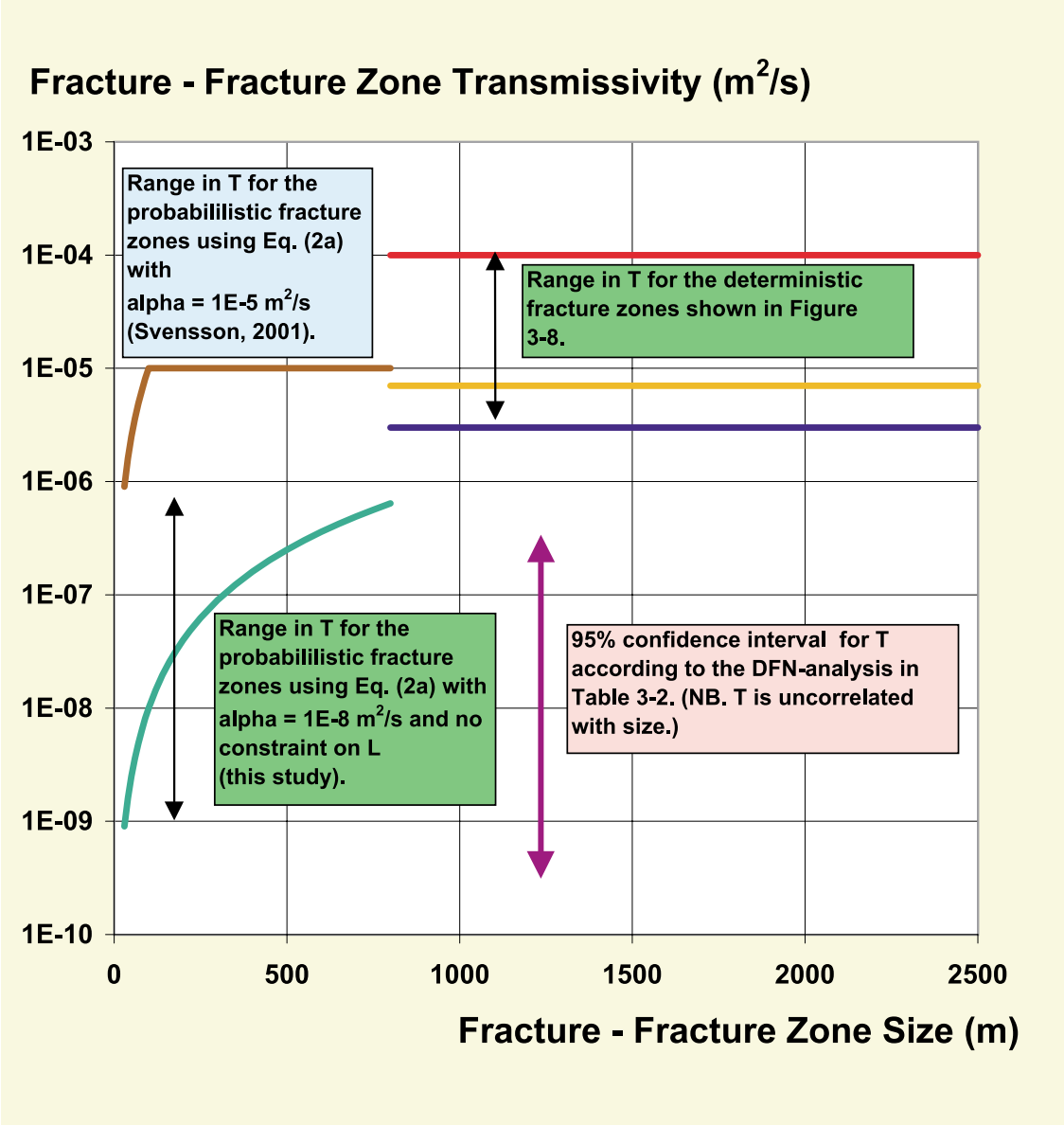

Figure 3-11. *Visualisation of the different proposals for the definition of fracture transmissivity discussed in this study.*

Concerning the derivation of the continuous field of low conductivities, the present study has adopted the assumption of a log normal distribution for $log_{10}K_{30} \in N(-10, 1)$ log_{10}(m/s) used in the Prototype repository model by /Svensson, 2001/. The main motive for this simplification was the constrained timetable of the project.

Concerning the derivation of the discrete field of high conductivities, Chapter 2 briefly describes the technique used in DarcyTools to transform fracture zone transmissivities to inter-node cell conductivities. For a more vivid description of this technique, the reader is kindly referred to /Svensson et al, 2002/.

Figure 3-12 illustrates the relative strength of the three sources that contribute to the derivation of the equivalent inter-node conductivity field in the Laxemar model domain. The conductivity realisation shown in Figure 3-13 demonstrates how the superposition of the deterministic and probabilistic sources may look.

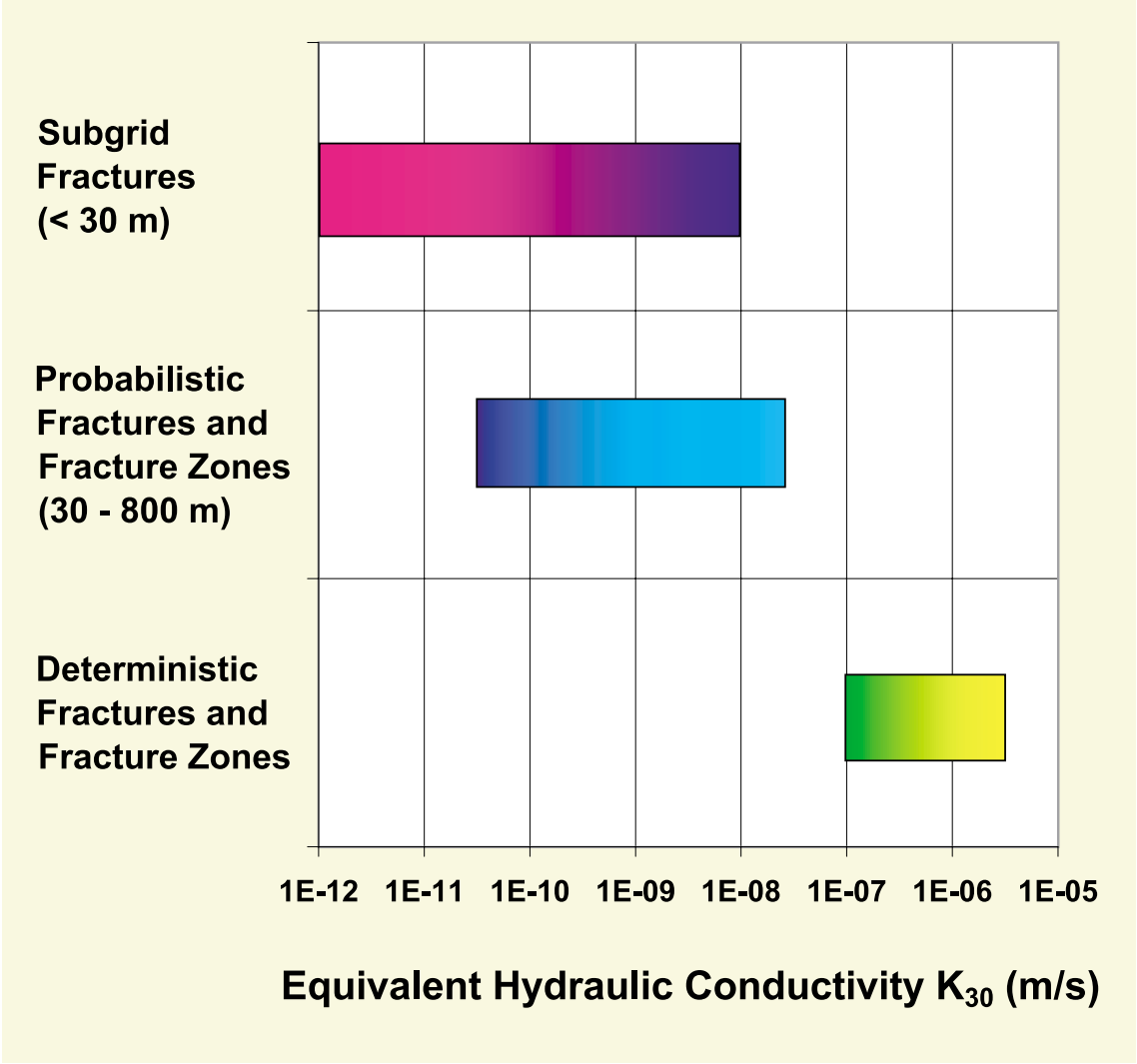

Figure 3-12. *Schematic illustration of the variability of the different sources that contribute to the derivation of the equivalent inter-node conductivity field in the Laxemar model domain. The grid size of the numerical flow model is 30 m.*

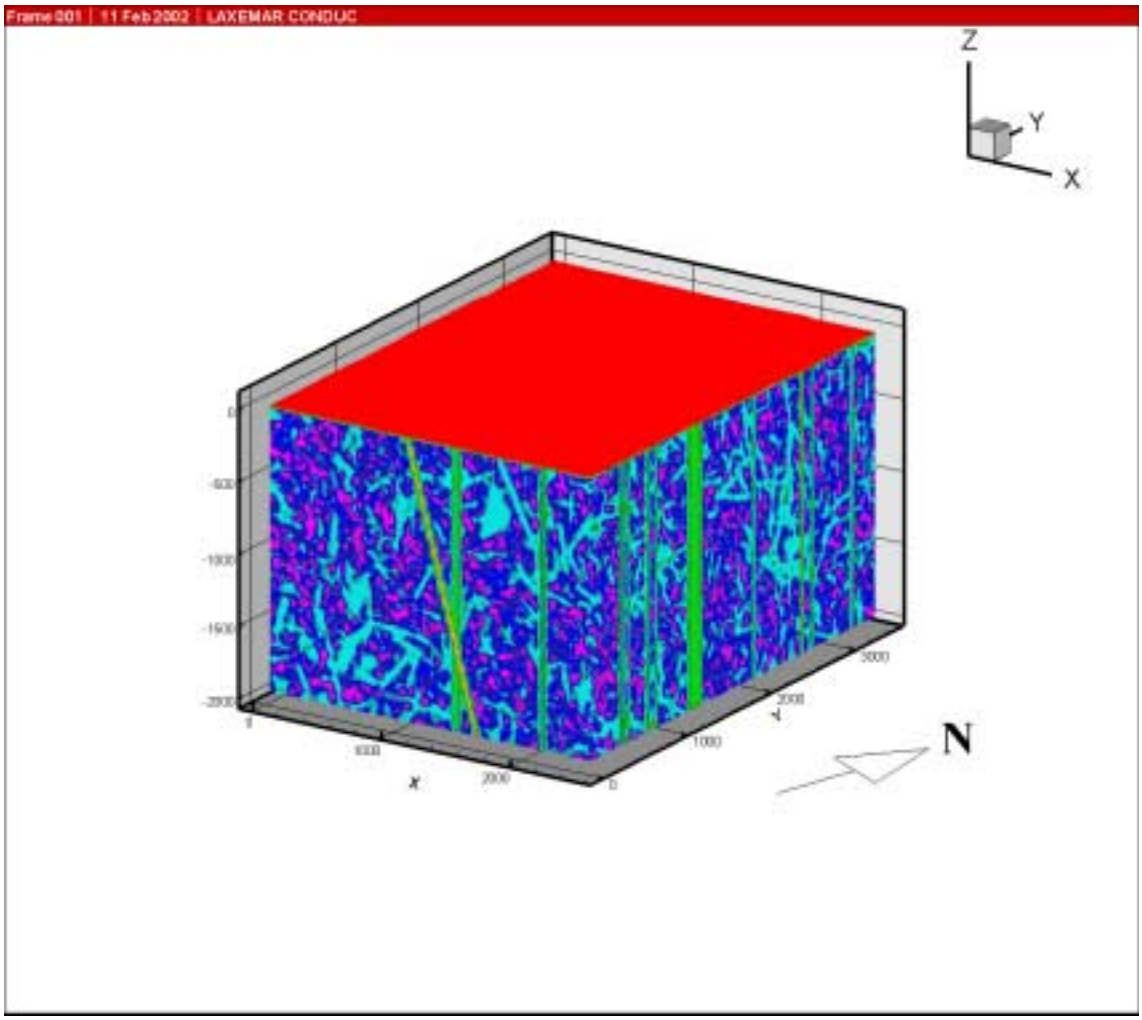

Figure 3-13. *3D visualisation of a conductivity realisation of the Laxemar model domain. The realisation is obtained by mean of superposition of deterministic and probabilistic sources. The colouring in the figure represents the contribution from four different sources. Three of these (purple-blue, turquoise and green-yellow) represent different types of bedrock structures, see Figure 3-12. The fourth (red), represents high conductivities close to the surface, e.g. Quaternary deposits.*

The hydraulic conductivity of the Quaternary deposits within the Laxemar area is briefly discussed in Section 3-6 of the methodology test report. No measurements of the hydraulic properties of the Quaternary deposits have been made. As indicated in Figure 3-1, however, exposed bedrock or bedrock with a very thin layer of Quaternary deposits, mostly till, dominate the area. Hence, it is likely that the surface runoff component of the net precipitation is large and the groundwater recharge to the bedrock is small.

For the purpose of this project, the hydraulic conductivity of the uppermost four layers of the numerical flow model were used to tune the position of the water table, which in turn affects the surface runoff and groundwater recharge to the bedrock. The result of the trial and error calibration process is displayed in Chapter 4. In short, the calibrated hydraulic conductivity of the uppermost four layers varied between 2×10^{-3}–1×10^{-6} m/s with the highest value closest to the surface.

3.5 Data interpretations, analyses and modelling

The region where the Laxemar model area is located has been subjected to extensive *hydrogeological interpretations*, *analyses and modelling* during the past 15 years. The major part of the work has been carried out in support of SKB's investigations and modelling of the Äspö Hard Rock Laboratory /see Rhén et al, 1997/. The experiences gained from this field work is summarised in Section 3.7 of the methodology test report.

Another large body of work is the SR 97 project /SKB, 1999/. Of particular interest for the methodology test project is the SR 97 regional model study by /Svensson, 1997a/, see Figure 1-1. The original idea was to use the pressure and salinity solution of the SR 97 regional model study by /Svensson, 1997a/ as boundary conditions for the for the Laxemar model area. However, this setting would imply an unrealistic mass flux across the vertical and bottom boundaries of the numerical flow model since there is no coupling between the regional and local conductivity field. The main reason for this discrepancy in hydraulic conductivity is the significant improvement of the structural geology since mid 1990's.

Moreover, using specified salinity and pressure fields on all sides of the model domain would counteract one of the objectives of the methodology test project. The objective in mind is the ambition to test the evaluation of site specific information with the planned methodology for site descriptive modelling with its requirements on integration and consistency between different disciplines and its requirement on documentation of data exchange. Indeed, specified salinity and pressure fields on all sides of the model domain of the numerical flow model would imply a too strong constraint for the simulated salinity distribution within the model domain. Conclusively, the desired comparison between measured and simulated concentrations in the proximity of the two deep core-drilled boreholes would not be satisfactory.

Figure 3-14 shows a close-up of Figure1-1. The grey rectangle is the SR 97 regional model area and the yellow rectangle is the Laxemar model area. The top figure shows the boundary conditions that were used by /Svensson, 1997a/. The bottom figure shows the boundary conditions that have been used in the present study. The western boundary of the Laxemar model domain coincides with a local topographic ridge. The north and south boundaries almost coincide with the mouths of the two small watercourses, Mistraån to the north and Laxemarån to the south. The eastern boundary coincides with the shoreline of the Baltic Sea. As indicated in Figure 3-14, the same boundary conditions were used in both flow models for the salinity and pressure distributions versus depth. The top boundary in each model coincides with ground surface. It is modelled as a specified flux boundary with a net infiltration of 200 mm/year and no salinity in the terrestrial part. In the marine parts, the pressure was set to the hydrostatic pressure of the Baltic Sea and the salinity to 6‰. Finally, the normal flux across the bottom boundary in each model is set to zero. It should be noted that the thickness of the SR 97 regional model domain was set to 3 000 m, whereas the thickness of the Laxemar model domain was set to 2 000 m by the methodology test project group.

The governing equations for flow and salt have been solved for steady state conditions, which means that porosity has no impact on the solution and that there are no considerations to transients such as seasonal changes in groundwater recharge or shore level displacement. From a hydraulic point of view, the adopted boundary conditions will create a balance between fresh and saline groundwater that is not dependent on the geology within the domain. The soundness of this fact is scrutinised in the next Chapter, but it may be noted that the Ghyben-Herzberg relation is a balance of forces solely.

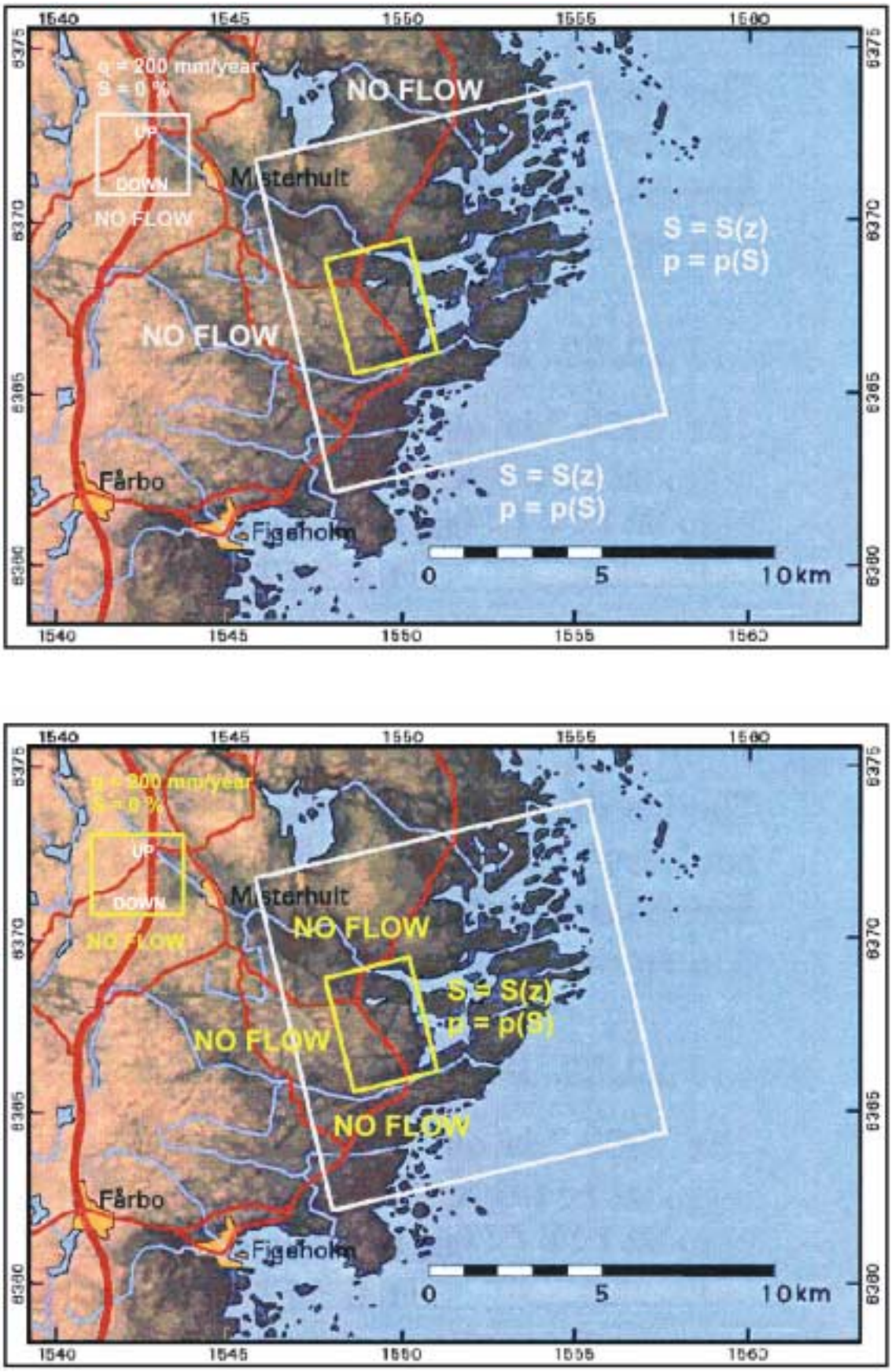

Figure 3-14. *The top figure shows the boundary conditions that were used in the SR 97 regional flow model by /Svensson, 1997a/. The bottom figure shows the boundary conditions of the present study. S = salinity, p = pressure and q = volumetric flux.*

4 Model calibration and simulation results

4.1 General

This chapter presents the results of a numerical exploration survey of the Site Descriptive Model set-up presented in Chapter 3. The set-up consists of three parts; the HCDs, which represents the deterministic structures of the Base geological model, the HRDs, which represents the heterogeneous rock mass in between and modelled by means of (*i*) probabilistic features in the size range 30–800 m, and (*ii*) a heterogeneous subgrid hydraulic conductivity field, the HSD, which represents the Quaternary deposits.

The numerical exploration survey is not detailed due to the limitations in the scope of the methodology test project. The intention has been to identify potential needs for development and improvement in the planned modelling methodology and tools. Hence, the conclusions that may be drawn from this study are mainly of general interest.

There are two important limitations of the numerical simulations that are of general interest. First of all, the Alternative geological model has not been dealt with, although it is recognised that the discrimination between provisional 'deterministic' geological models by means of exploration simulations is probably one of the more important tasks. Secondly, the handling of probabilistic features is solely unconditional[3] . The implications of working with solely unconditional realisations are discussed in Chapter 5.

The numerical exploration survey is divided into two parts. The first part treats the calibration of the unconditional realisations. Due to the constrained timetable of the methodology test project, the calibration has been restricted to treat two features and three realisations only. The second part checks the capability of the calibrated unconditional realisations of reproducing measured hydrogeological and hydrogeochemical data that were not used for the calibration. Hence, the second part may be regarded as some kind of creditability test of the Site Descriptive Model set-up.

4.2 Calibration

The calibration has been directed to treat two specific features, namely:

1. The coefficient α in the equation that relates fracture transmissivity to fracture size, see Equation 6 in Chapter 2. The value of α was altered until a reasonable agreement was obtained between the *CDF* of the inter-node hydraulic conductivity field in the flow model and the *CDFs* of the K_{30} measurements carried out in the two deep core-drilled boreholes KLX01 and KLX02.

[3] Unconditional realisations honour the ensemble statistics of the available local geometric and hydraulic properties, but not the local properties as such. The process of honouring local properties, e.g. borehole transmissivities at specific locations, is called conditioning. Conditioning is discussed in Chapter 5.

2. The hydraulic conductivity K of the uppermost four cell layers of the flow model. The value of K was tuned for each layer (without changing the transmissivities of the HCD and HRD) until a reasonable agreement was obtained between simulated and known surface water conditions within the entire Laxemar model domain.

The first feature was chosen because of the presumed importance of probabilistic fractures and fracture zones for the hydraulic conductivity of the bedrock and the groundwater flow distribution at depth. The second feature was chosen because of the extreme importance of the top boundary condition.

4.2.1 Hydraulic conductivity at depth

Figure 4-1 shows five graphs that represent different cumulative density functions (CDFs) for the hydraulic conductivity of the bedrock on a 30 m support scale (K_{30}). Three of the five CDFs represent field data (light green, cerise and red) measured between c. 100 m–1 660 m in the specified core-drilled boreholes, KLX01, KLX02 and KAS02–03. The remaining two CDFs (blue and dark green) are numerical simulations of K_{30}, denoted by DT_C-1 and DT_C-2. Each realisation consists of three sources of data; the deterministic fracture zones of the Base geological model, a Monte Carlo simulation of probabilistic fractures and fracture zones and a Monte Carlo simulation of a heterogeneous subgrid hydraulic conductivity field. Figure 3-13 shows an example of such a realisation in 3D.

The two CDFs representing Laxemar data are not entirely alike, but their median values are c. one order of magnitude less than the median of the CDF representing Äspö data. Hence, the CDFs indicate that hydraulic differences may exist between the two areas.

The K_{30} realisations DT_C-1 and DT_C-2 are geometrically identical but differ in the value of the coefficient that relates transmissivity to fracture size. That is, the simulation DT_C-1 has an α-value of 10^{-5} m^2/s whereas DT_C-2 has an α-value of 10^{-8} m^2/s. Given the used equations, Figure 4-1 indicates that probabilistic fractures have a significant impact on the bedrock hydraulic conductivity and the groundwater flow distribution at depth. It should be noted, however, that this study merely points at the importance of the issue without making any real attempt to address it as such. Indeed, the DFN-analyses in Section 3.8 of the methodology test report do not address whether there is a positive correlation between fracture transmissivity and fracture size of the kind used in this study.

The other two unconditional realisations of this study, DT_C-3 and DT_C-4, are geometrically different from each other and from DT_C-2. Despite their geometric differences, however, the CDFs of the three unconditional realisations are quite alike, which implies that the size of the Laxemar model domain is sufficiently large in order to appeal to this type of ergodicity test.

The deviation in the upper part of the CDF that represents the hydraulic testing in KLX01 is interesting and important. As will be shown later, the deviation is due to high conductivity values in the uppermost part of KLX01.

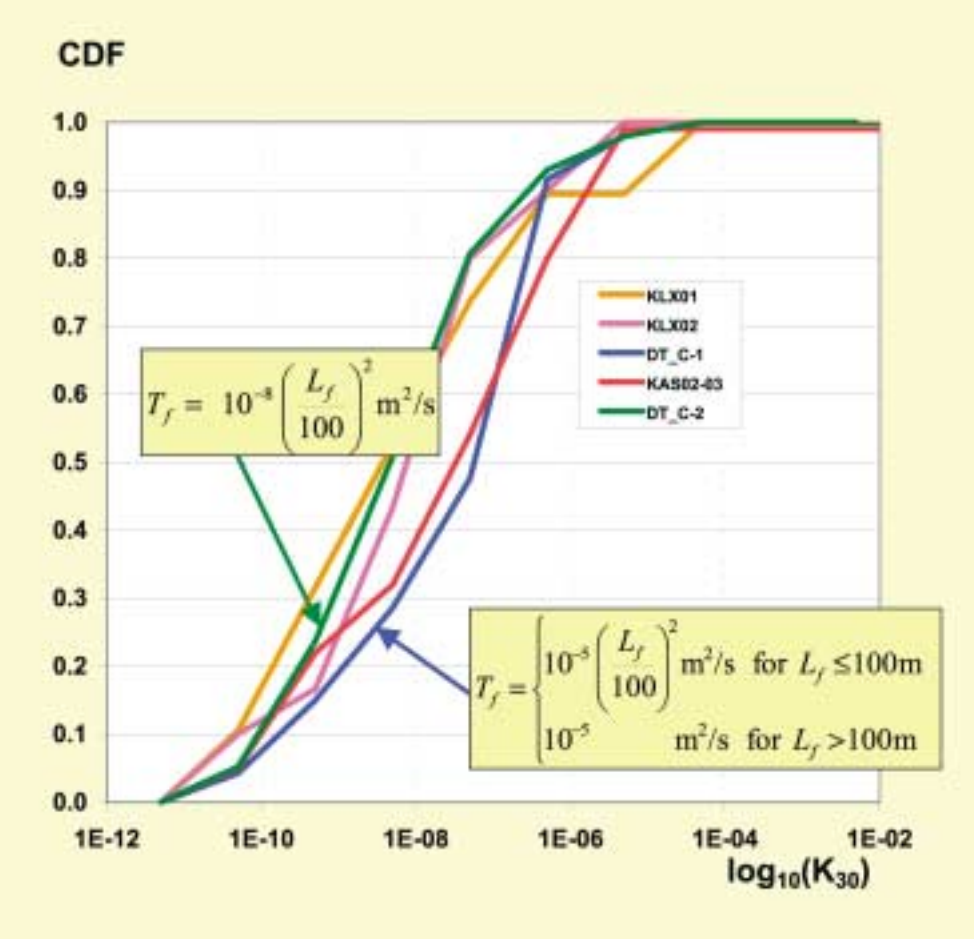

Figure 4-1. *Cumulative density functions (CDFs) for the hydraulic conductivity on a 30 m support scale. The CDFs denoted by DT_C-1 and DT_C-2 are based on simulations with DarcyTools and the CDFs denoted by KLX01, KLX02, and KAS02–03 are based on single-hole measurements between 100–1 660 m.*

4.2.2 Hydraulic conductivity close to ground surface

The hydraulic conductivity of the uppermost layers of a numerical flow model in DarcyTools may be used to tune the position of the water table and hence the spatial distribution of recharge and discharge areas. If the hydraulic conductivity of the uppermost layer is high, saturated grid cells in the topographic lows will form a flow pattern that resembles the surface hydrological conditions, i.e. wetlands, lakes and streams. Unfortunately, the present knowledge about the hydrology of the Laxemar area is quite limited. Except for the elevation of Lake Frisksjön, there are no other hydrological data to calibrate against. According to Figure 3-1, however, the uppermost part of the subsurface consists of a thin layer of flushed till or outcropping bedrock, which suggests that the surface runoff should be quite high.

The values of the hydraulic conductivity of the uppermost four layers of the numerical flow model were altered until the size of Lake Frisksjön was mimicked, see Figure 4-2. The calibration was simplified by keeping the hydraulic conductivity of each layer constant throughout the model domain. The final conductivity values varied between 2×10^{-3}–1×10^{-6} m/s with the highest value closest to the surface. The thickness of the four layers was programmed to follow a power law series of $\tau\times2^{(n-1)}$, with n=1 for the uppermost layer and a $\tau\approx1.6$ m. Figure 4-2 is valid for all three realisations as the contrast in hydraulic conductivity between the upper and lower parts of the flow system is quite large, see Figure 4-1.

The performed tuning of the hydraulic conductivity of the uppermost layers carried out in support of this project is by no means exhaustive. The point made here is that the hydrogeological conditions on the top boundary are important for the creditability of the environmental impact assessment. Questions like "How large will the radius of influence be once the construction of the deep repository has started?" require a good understanding of the conditions that govern the relation between the net precipitation and the maximum groundwater recharge. Conclusively, it is important to have a good control of surface runoff parameters such as lake elevation verges and stream flow rates, but also the thickness and conductivity of the Quaternary deposits.

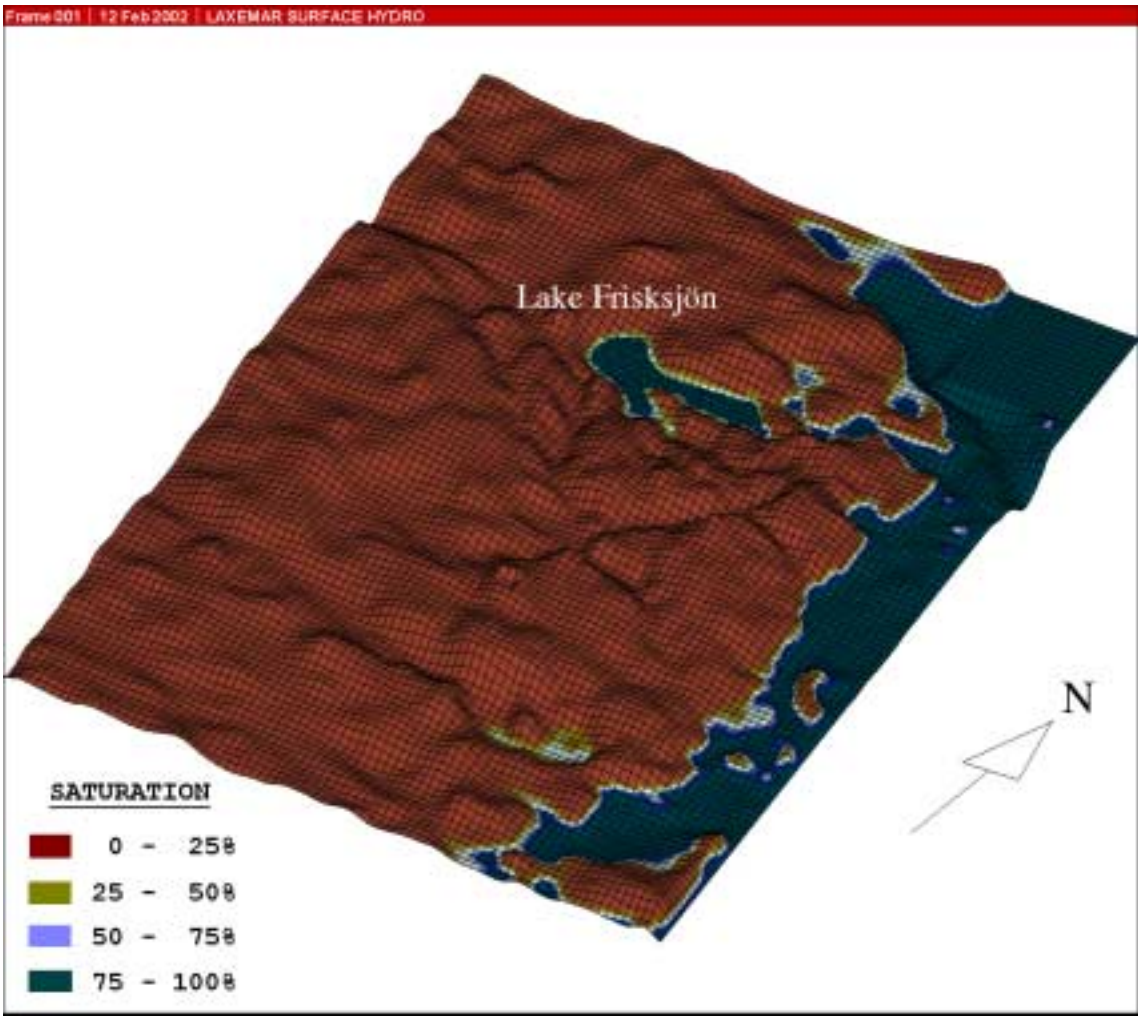

Figure 4-2. *Visualisation of the saturation of the uppermost layer in the numerical flow model of the Laxemar model area. The values of the hydraulic conductivity of the uppermost layers of the numerical flow model were chosen so that the size of Lake Frisksjön was approximately correct, cf. Figure 3-5.*

4.3 Numerical simulations

4.3.1 Hydrogeological evaluation

The results from the 35 days long interference test conducted between drillhole KLX02 (pumping hole) and KLX01 (observation hole) in 1996 /Follin, 1996/ was chosen by the methodology test project team as a reference test for the numerical exploration of the "calibrated" flow model. Due to the constrained timetable it was decided to work with one of the three realisations only for the numerical simulation of the interference test.

In order to make the numerical simulation of the interference test as realistic as possible from a hydraulic-structural point of view, it was decided to work with the realisation that had the closest simulated test section transmissivity value with regards to the real value in the pumped borehole, KLX02. In this way, an erratic drawdown and a subsequent erratic saltwater upconing effect at the origin for the pressure disturbance would be avoided. However, it should be stressed that the taken approach is unsatisfactory from a conditional point of view since the local information at the observation borehole, KLX01, is not taken into account. Possible means of avoiding this artefact while working with unconditional realisations was discussed by the methodology test project team. However, it was decided to push this important issue to the discussions on uncertainties, see Chapter 5. Hence, no efforts were made to treat the problem within the scope of methodology test project. Table 4-1 shows a comparison between the different test section transmissivities in the pumped borehole KLX02 and the observation borehole KLX01.

Figures 4-3 and 4-4 show the measured and simulated K_{30} values along the stretch of the two boreholes KLX02 and KLX01. K_g denotes the geometric mean of the simulated directional cell wall conductivities K_{x+}, K_{y+}, K_{z+}, K_{x-}, K_{y-} and K_{z-} (cf. Chapter 2). The blue graphs represent "measured" K_{30} values. For KLX02, the K_{30} values were deduced by lumping ten subsequent 3 m transmissivity values (determined by the PFL method) and divide the sum by 30 m. For KLX01, the K_{30} values were obtained by means of 30 m double-packer injection tests. There are no data below 673 m depth in borehole KLX01.

Table 4-1. Comparison between the different test section transmissivities in the pumped borehole KLX02 and the observation borehole KLX01. C2–C4 are realisations. Realisation C3 was chosen for the simulation of the interference test. /Follin, 1996/ is the source for the estimated transmissivity of the test section in KLX02, whereas /Follin, 1993/ is the source for the corresponding values in KLX01.

Borehole Test section interval	Estimated Transmissivity	Transmissivity of Real. C2	Transmissivity of Real. C3	Transmissivity of Real. C4
KLX02 *805–1103 m*	5.7×10^{-6} m²/s	4.3×10^{-8} m²/s	5.1×10^{-6} m²/s	1.5×10^{-7} m²/s
KLX01 – A *0–140 m*	6.2×10^{-5} m²/s	5.3×10^{-7} m²/s	8.2×10^{-8} m²/s	1.7×10^{-7} m²/s
KLX01 – B *141–271 m*	6.2×10^{-5} m²/s	3.5×10^{-8} m²/s	4.2×10^{-8} m²/s	4.3×10^{-7} m²/s
KLX01 – C *272–694 m*	6.2×10^{-5} m²/s	1.2×10^{-7} m²/s	1.0×10^{-6} m²/s	3.1×10^{-7} m²/s
KLX01 – D *695–855 m*	1.1×10^{-5} m²/s	6.1×10^{-6} m²/s	1.5×10^{-5} m²/s	6.1×10^{-6} m²/s
KLX01 – E *856–1 078 m*	4.0×10^{-6} m²/s	9.0×10^{-6} m²/s	3.9×10^{-7} m²/s	9.0×10^{-6} m²/s

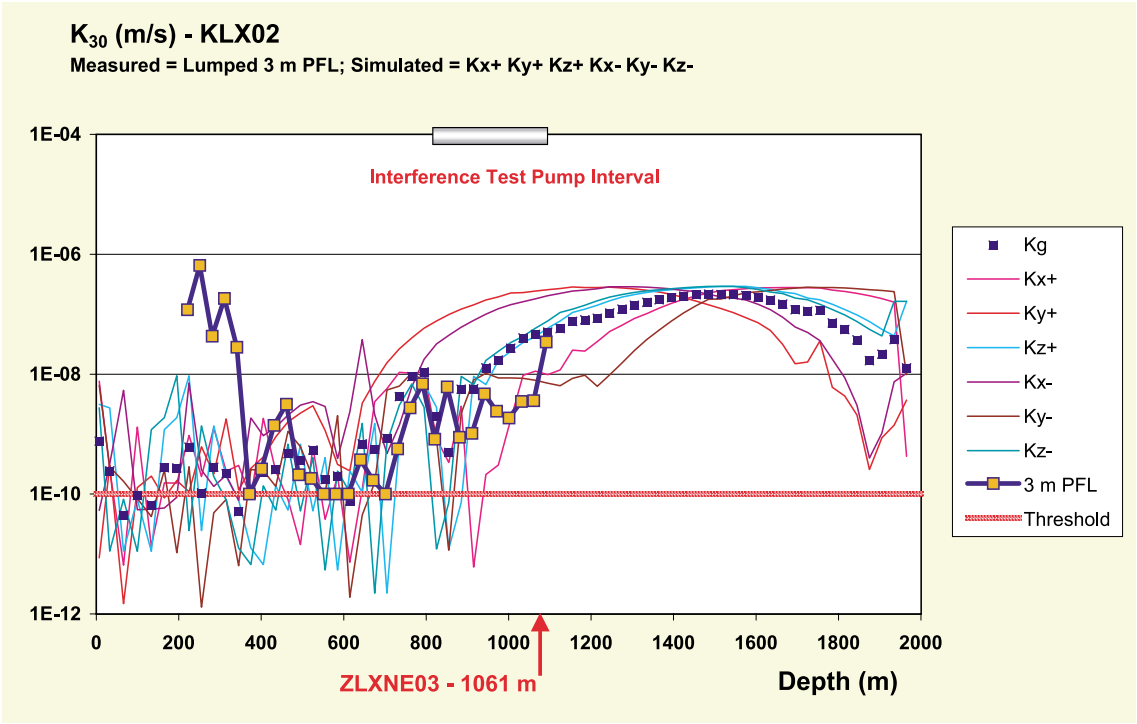

Figure 4-3. *Measured and simulated K_{30} values in the pumped borehole KLX02. The intersection between the borehole and the fracture zone ZLXNE03 is indicated by the red arrow. The fracture zone is c. 15 m wide and sub-parallel with the borehole inclination.*

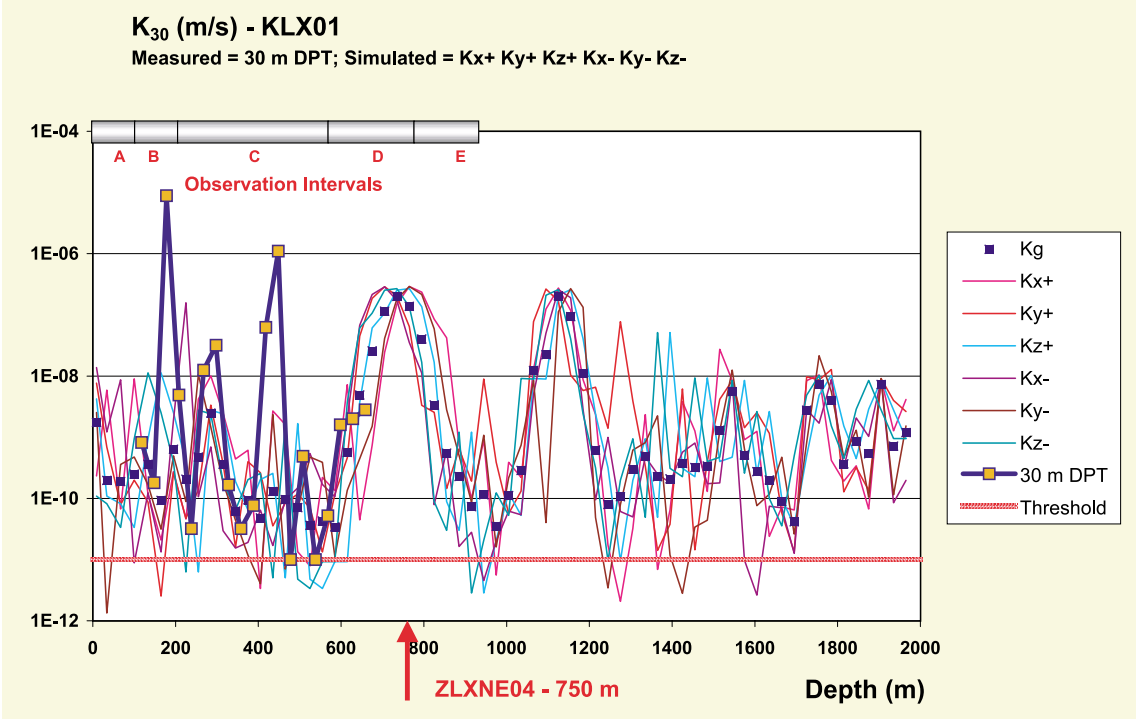

Figure 4-4. *Measured and simulated K30 values in the observation borehole KLX01. The intercept of the fracture zone ZLXNE04 is indicated by the red arrow. The fracture zone is c. 15 m wide and dipping in an opposite direction to the borehole inclination, which is c. 87°.*

Borehole KLX02 is intersected by zone ZLXNE03 at c. 1 061 m. The zone is interpreted to be c. 15 m wide and sub-parallel with the borehole inclination. The dip angles are 87° and 85° respectively. The proximity of the zone shows up in the measurements as well as in the simulation as a persistent elevation of the corresponding data.

The measured hydraulic conductivity in the upper part of KLX02 between 200–300 m is not captured by the studied realisation. Obviously, a geometric structure with a fairly high transmissivity is missing in the Base geological model at this position. In contrast, the Alternative geological model contains a sub-horizontal fracture zone at this depth, ZLXEW02, see Figure 3-3. Zone ZLXEW02 has an inclination of 49° N. It should be noted that the Alternative model is not constructed on the basis of the measured hydraulic anomalies but on an interpretation of the reflection seismic anomalies. The correlation with the hydraulic data makes the Alternative model very interesting.

In the Base geological model, borehole KLX01 is intersected by zone ZLXNE04 at c. 750 m. The interpreted intersection is based solely on geological data since there are no hydraulic measurements at this depth to support the interpretation. The zone ZLXNE04 is interpreted to be c. 15 m wide and dips 72°. Since borehole KLX01 is almost vertical, the peak in the simulated hydraulic data is fairly sharp, see Figure 4-4.

There are several positions in the upper part of KLX01 where the hydraulic measurements are not well captured by the studied realisation, e.g. at 180 m, 260 m and 420 m. In the Alternative geological model, the dip angle of zone ZLXNE04 is changed to 59° due to the interpretation of the reflection seismic anomalies. The alternative interpretation alters the intersection with KLX02 to c. 420 m, where one of the major hydraulic anomalies is located.

At c. 1 100 m there is another sharp peak in the simulation. Since there are no measurements made below 673 m, the correctness of this peak can not be concluded. However, there is no fracture zone in the Base geological model that intersects the borehole at this depth, which means that the simulated values stems from a probabilistic fracture zone.

4.3.2 Numerical simulation of an interference test

Figure 4-5 illustrates the model set-up for the simulation of the interference test. The pumping rate in borehole KLX02 is set to 9 L/min and the duration of the interference test is 35 days. The length of the pumped interval in KLX02 is almost 300 m. There are five observation intervals in borehole KLX01, A–E, see Table 4-1. The execution and interpretation of the interference test is described in /Follin, 1996/, who in turn partly refers to the evaluation of the open borehole interference test conducted in 1992–93 and reported by /Follin, 1993/. Figure 4-6 shows the monitored responses in the freshwater head in the five observation intervals in borehole KLX01 during the considered test period. According to /Follin, 1996/, the interference test reached almost stationary drawdown conditions during the test period.

Figure 4-7 shows an X-ray view of the simulated steady state drawdown of the freshwater head. The drawdown is plotted for a vertical cross-section running through the two boreholes KLX02 and KLX01.

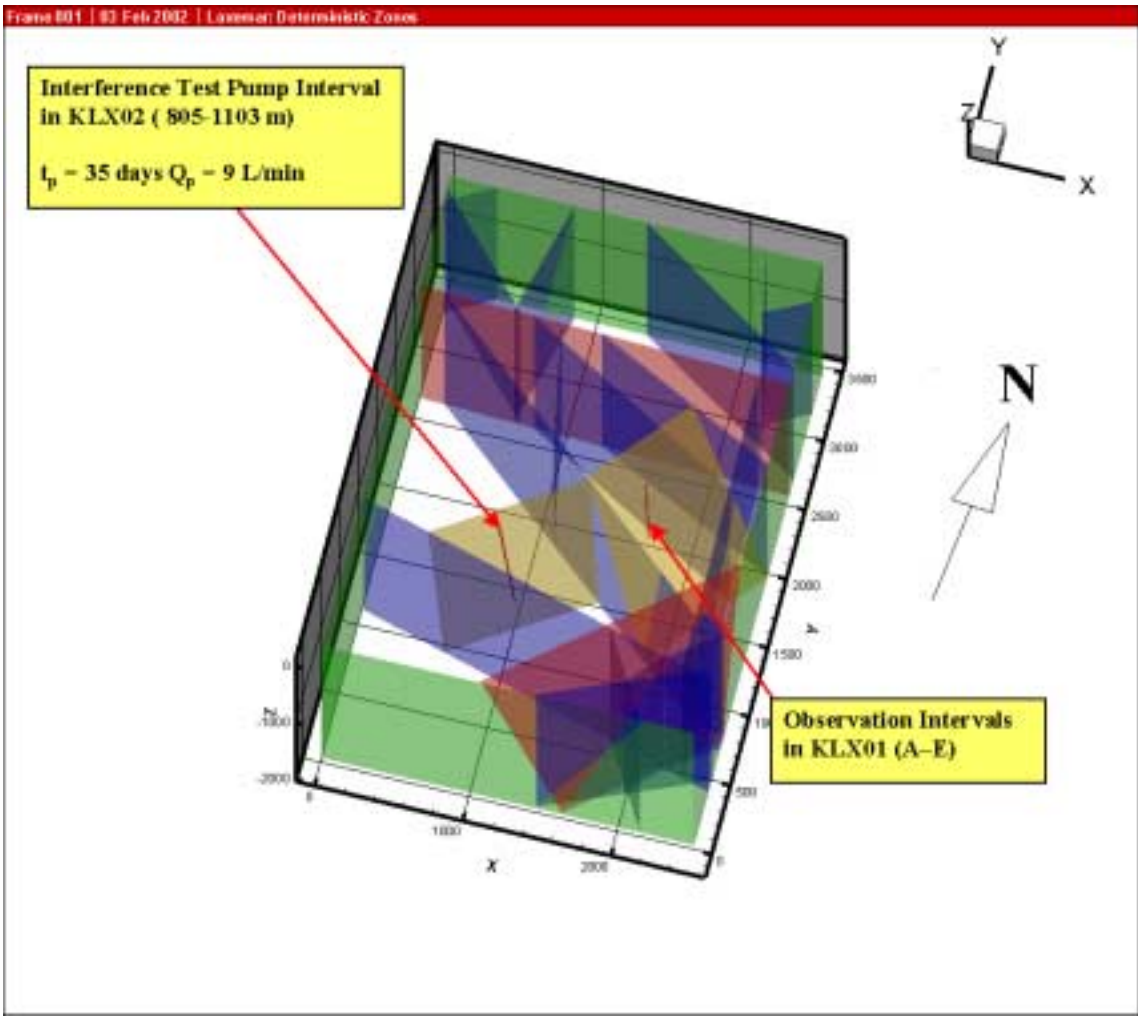

Figure 4-5. *Isometric visualisation of the interference test configuration.*

Figure 4-8 also shows the simulated steady state drawdown in the freshwater head. The drawdown is presented in five horizontal cross-sections coinciding with the centre of each observation interval, A–E. Figures 4-6 and 4-7 imply that the propagation of a steady state pressure field around the pumped borehole is not narrowed to the deterministic zones. Moreover, the size of the model domain in combination with the used boundary conditions is found to constrain the propagation of the drawdown to the west.

Table 4-2 shows the measured and simulated drawdown values in the freshwater head in the observation borehole KLX01. The order of magnitude in the simulated drawdown appears to be correct, which indicates that the overall calibration of the probabilistic zones presented in Figure 4-1 can be defended given the limitations at the time of the methodology test project. The major discrepancies between the measured and simulated drawdown values are observed in observation intervals D and E, which is not surprising given the status and derivation of the Base geological model and the lack of conditioning of the studied realisation.

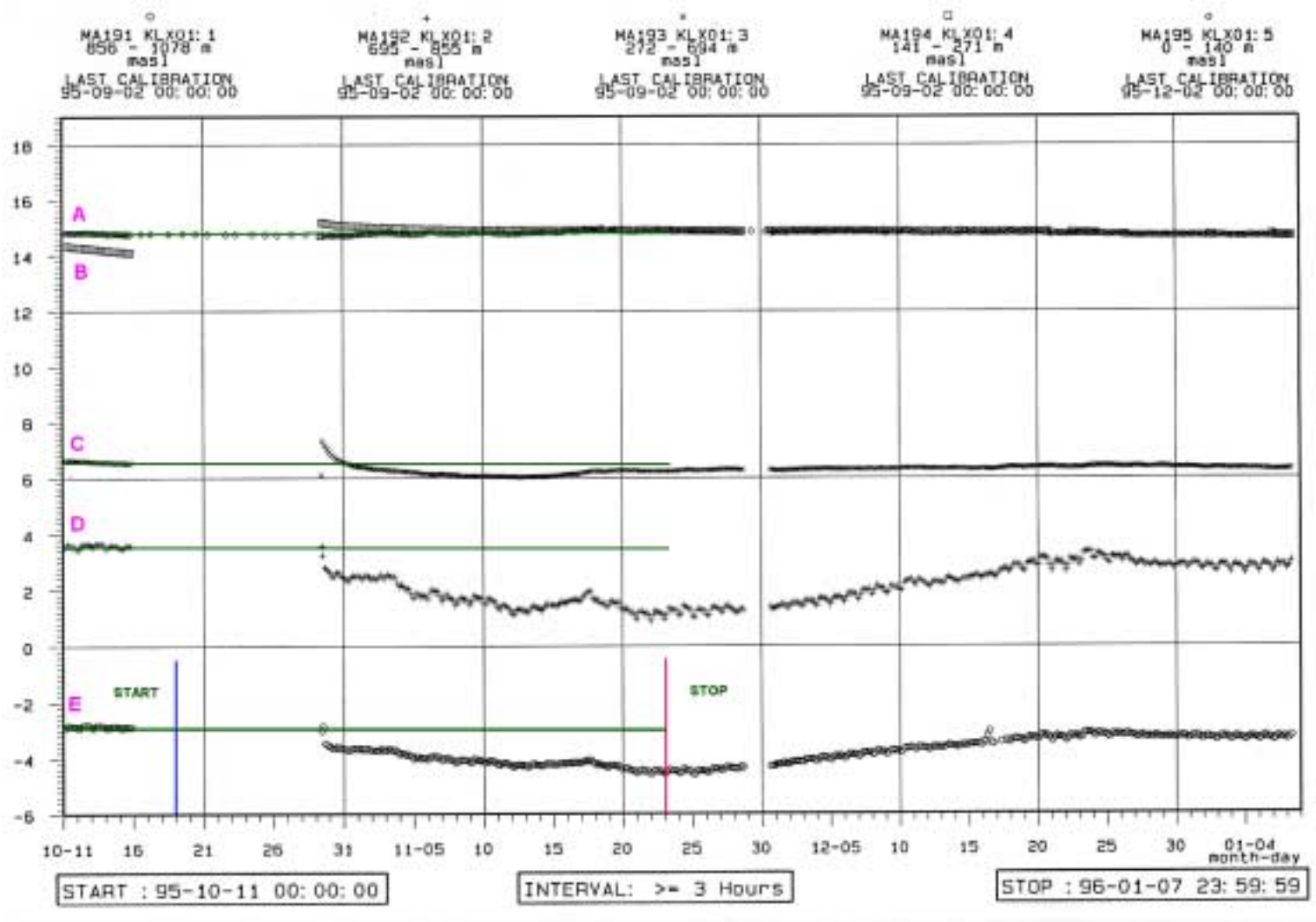

Figure 4-6. *Monitored responses in the freshwater head in the five observation intervals, A–E, in borehole KLX01 during the considered interference test /Follin, 1996/. The monitoring indicates pseudo-stationary drawdown conditions at the end of the 35 day long test period.Figure 4-7 shows an X-ray view of the simulated steady state drawdown of the freshwater head. The drawdown is plotted for a vertical cross-section running through the two boreholes KLX02 and KLX01.*

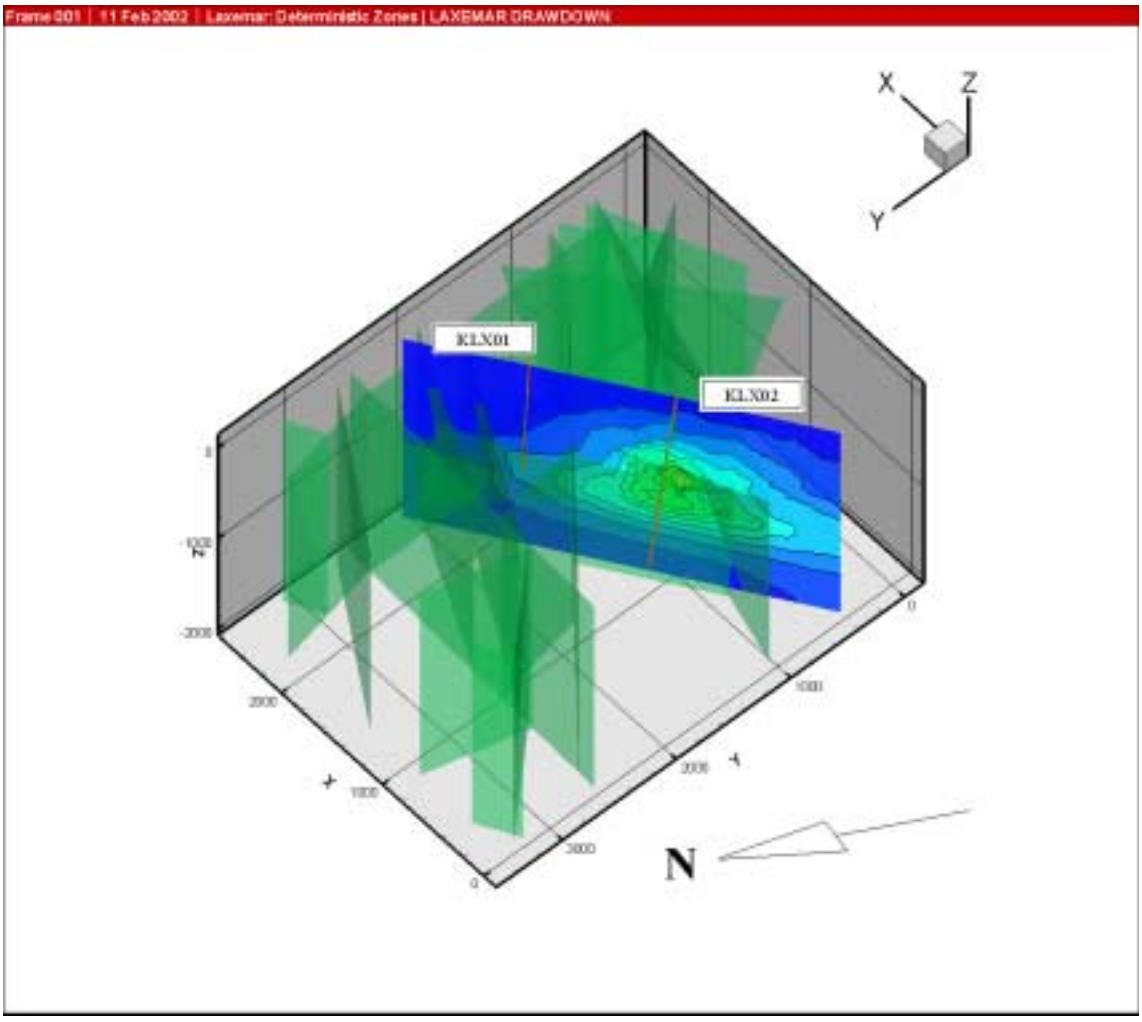

Figure 4-7. *Visualisation of the drawdown in a vertical cross-section running through the two boreholes (KLX02 to the right). The green surfaces represent the deterministic zones of the Base geological model.*

Tabell 4-2. Comparison between measured and simulated drawdown values in the freshwater head in the observation hole KLX01.

Test Section	Measured drawdown in freshwater head	Simulated drawdown in freshwater head
KLX01, A: 0–140 m	~0 m	0.15 m
KLX01, B: 141–271 m	~0 m	0.23 m
KLX01, C: 272–694 m	0.6 m	0.83 m
KLX01, D: 695–855 m	2.3 m	1.07 m
KLX01, E: 856–1078 m	1.5 m	2.12 m

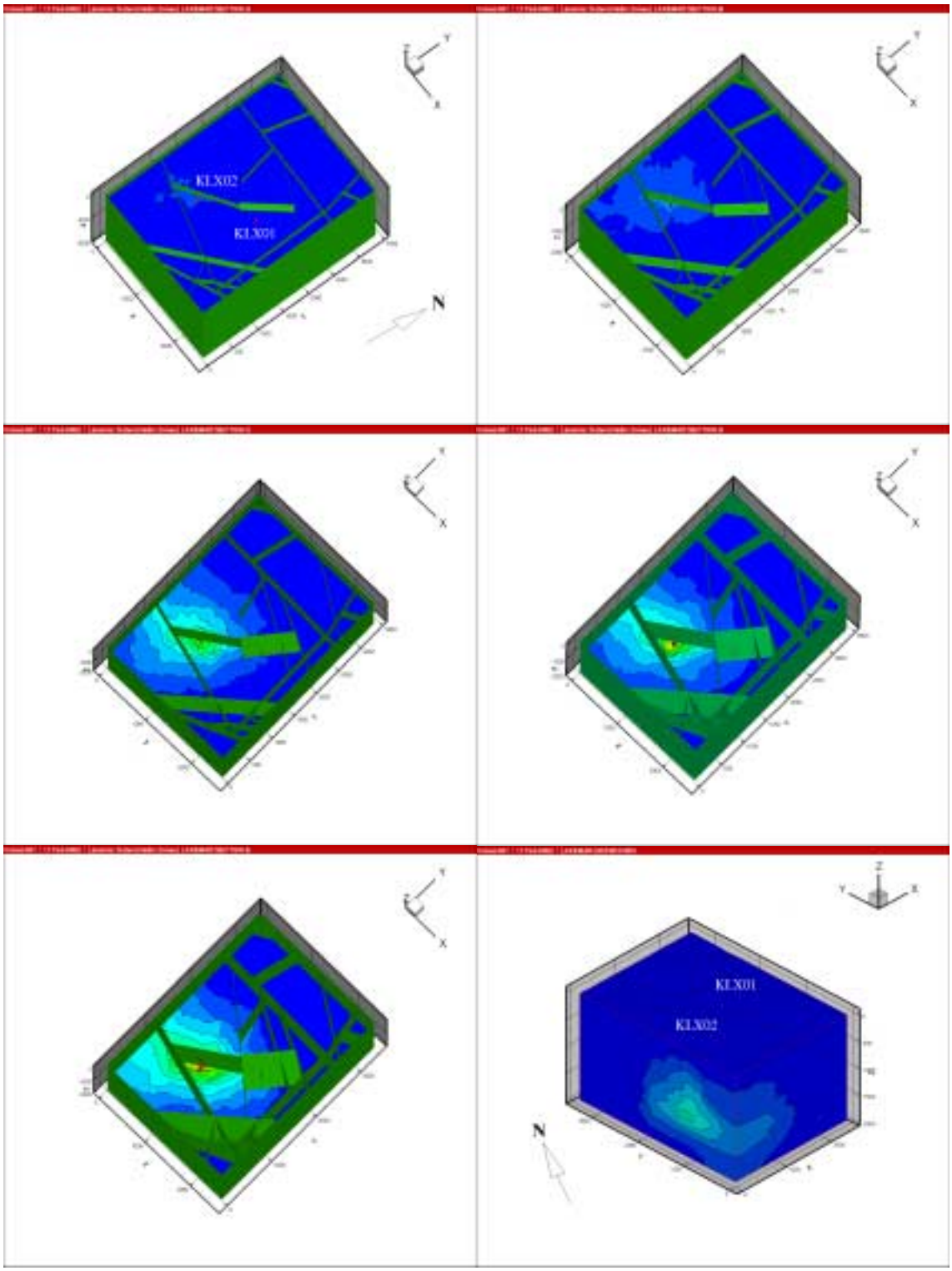

Figure 4-8. *Simulated steady state drawdown in the freshwater head. The insets show the drawdown in five horizontal cross-sections coinciding with the centre of each observation interval, A–E. The inset to the right at the bottom row shows the intersection of the simulated drawdown with the western and southern no-flow boundaries of the model domain.*

4.3.3 Hydrogechemical evaluation

The hydrogeochemical evaluation of the numerical flow model has been focused on the simulated distribution of saline groundwater. The evaluation was divided into four steps:

1. Comparison between the three realisations C2–C4.
2. Comparison between the simulated salinity distribution along the western no-flow boundary of the Laxemar model domain with the free node solution at the same location in the regional flow model by /Svensson, 1997a/.
3. Comparison between the measured salinity profiles in boreholes KLX01 and KLX02 and the simulated salinity profiles at the corresponding locations in the flow model.
4. Comparison between the measured and simulated upconing effects during the studied inference test.

Comparison between the three realisations C2–C4

This step was carried out to check the consistency of the solver with regards to the three realisations. According to the Ghyben-Herzberg principle /Bear, 1979/, the balance between fresh and saline groundwater at *steady state* is independent of the geological conditions.

Figure 4-9 shows three vertical cross-sections corresponding to the three realisations C2–C4. Each cross-section shows the salinity distribution for a profile that runs through the two boreholes, KLX01 and KLX02. It is confirmed that the "geological differences" between the realisations have little or no impact on the solution and that the solver works as expected.

The salinity distribution along the western no-flow boundary of the Laxemar model domain

This step was carried out to study the effect of the imposed conditions on the western side of the model domain. Since the differences between the three realisations are negligible, the comparison was made for realisation C3 only.

Figure 1-1 shows the location of the Laxemar model domain with regards to the SR 97 regional model domain and the regional topographic gradient. The used boundary conditions for the two model domains are discussed in Chapter 3 and summarised in Figure 3-14.

Despite the differences in size and underlying conceptual geological conditions such as different geometries and hydraulic properties of the fracture zones, it may be advocated once more that the steady state assumption supersede the geological and boundary conditions. The salinity distribution is practically identical for the two models, see Figure 4-10, despite the fact that the western boundary is conceptualised as a no-flow boundary in the Laxemar model.

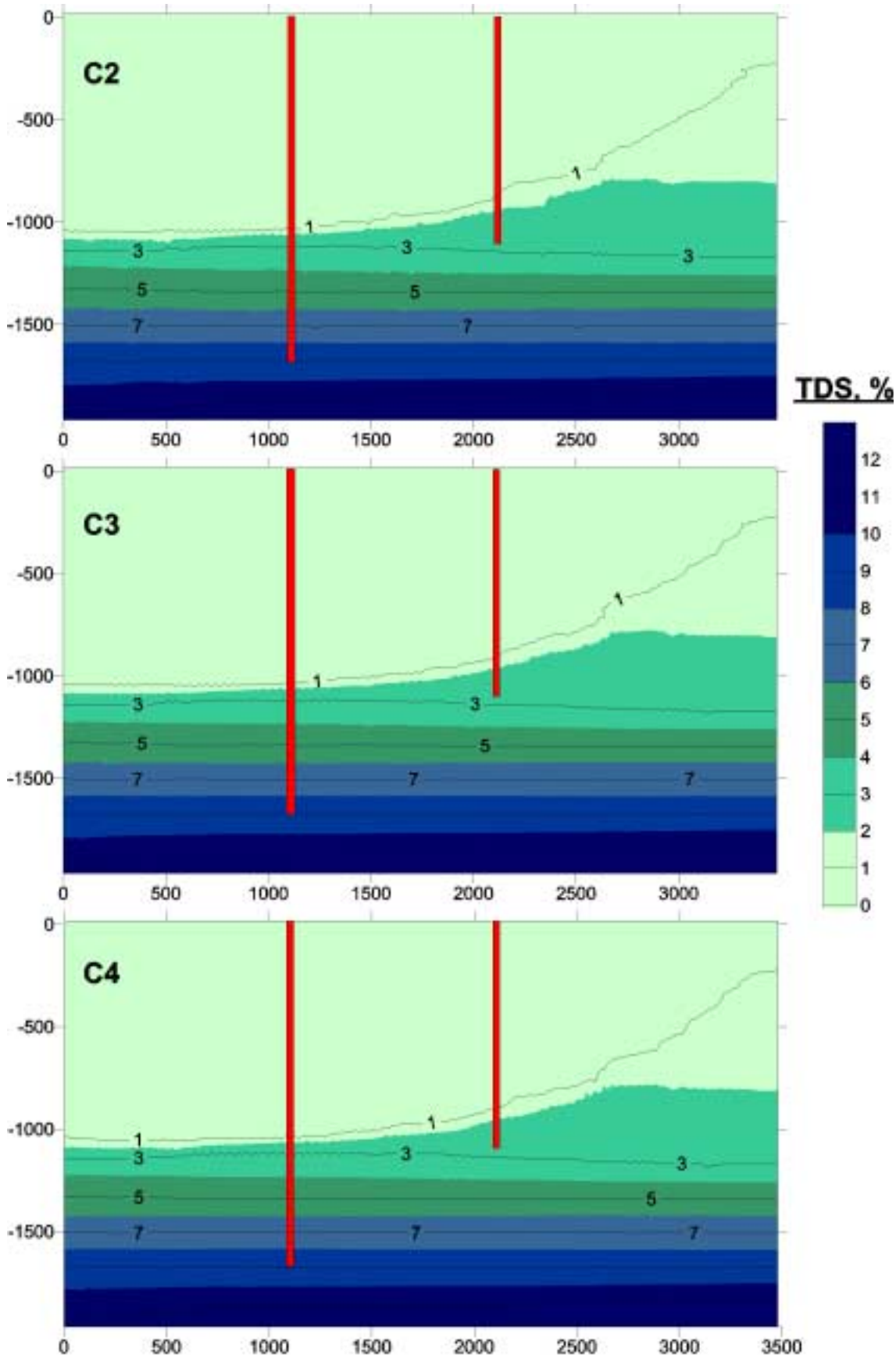

Figure 4-9. *Vertical cross-sections showing the steady state salinity distribution for a profile that runs through the two boreholes, KLX01 and KLX02. C2–C4 are three realisations with different geological conditions.*

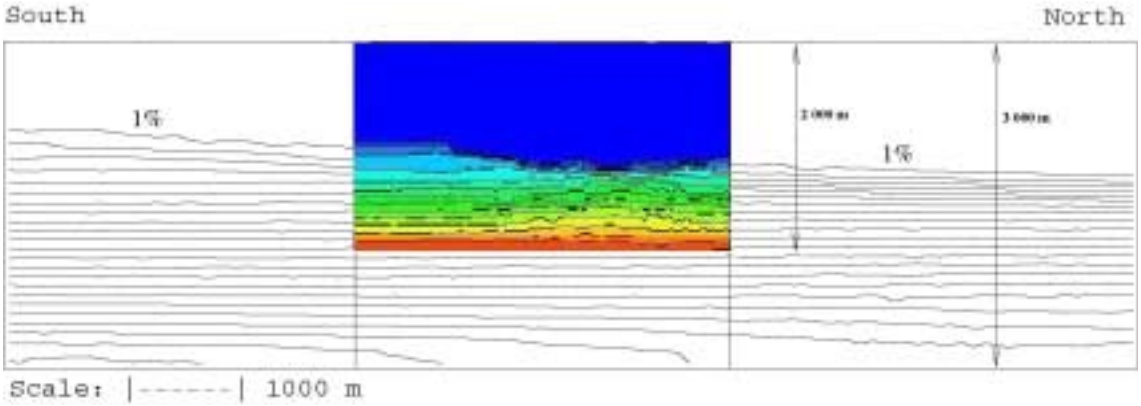

Figure 4-10. *Comparison between the simulated salinity distribution along the western no-flow boundary of the Laxemar model domain with the free node solution at the same location in the regional flow model by /Svensson, 1997a/. The coloured inset shows the salinity distribution for the Laxemar model, whereas the black and white figure in the background is the salinity distribution obtained from the SR 97 regional flow model.*

Comparison between measured and simulated salinities in boreholes KLX01 and KLX02

In order to facilitate the comparisons with the SR 97 regional flow model for Äspö /Svensson, 1997a/, the methodology test project team decided to use the same prescribed salinity distribution versus depth on the eastern side of the model domain as that of the SR 97 regional flow model. According the documentation of the Äspö HRL project /Rhén et al, 1997/, the used salinity distribution renders a salinity of c. 12% at 2 000 m depth. However, according to the hydrogeochemical description of the Laxemar area, the deepest measurements in borehole KLX02 (c. –1 440 m.a.s.l.) indicate that the salinity at 2 000 m depth should not exceed c. 8.5%. Despite this ambiguity in the salinity distribution, Figure 4-11shows that the simulated and measured positions of the freshwater/saltwater interface is approximately correct, at least in the borehole KLX02, which suggests that Laxemar area may be close to pseudo-steady state c. 1.5 kilometres from the sea. The discrepancy between measured and assumed salinity gradients on the eastern boundary mainly affects the gradient below the simulated interface.

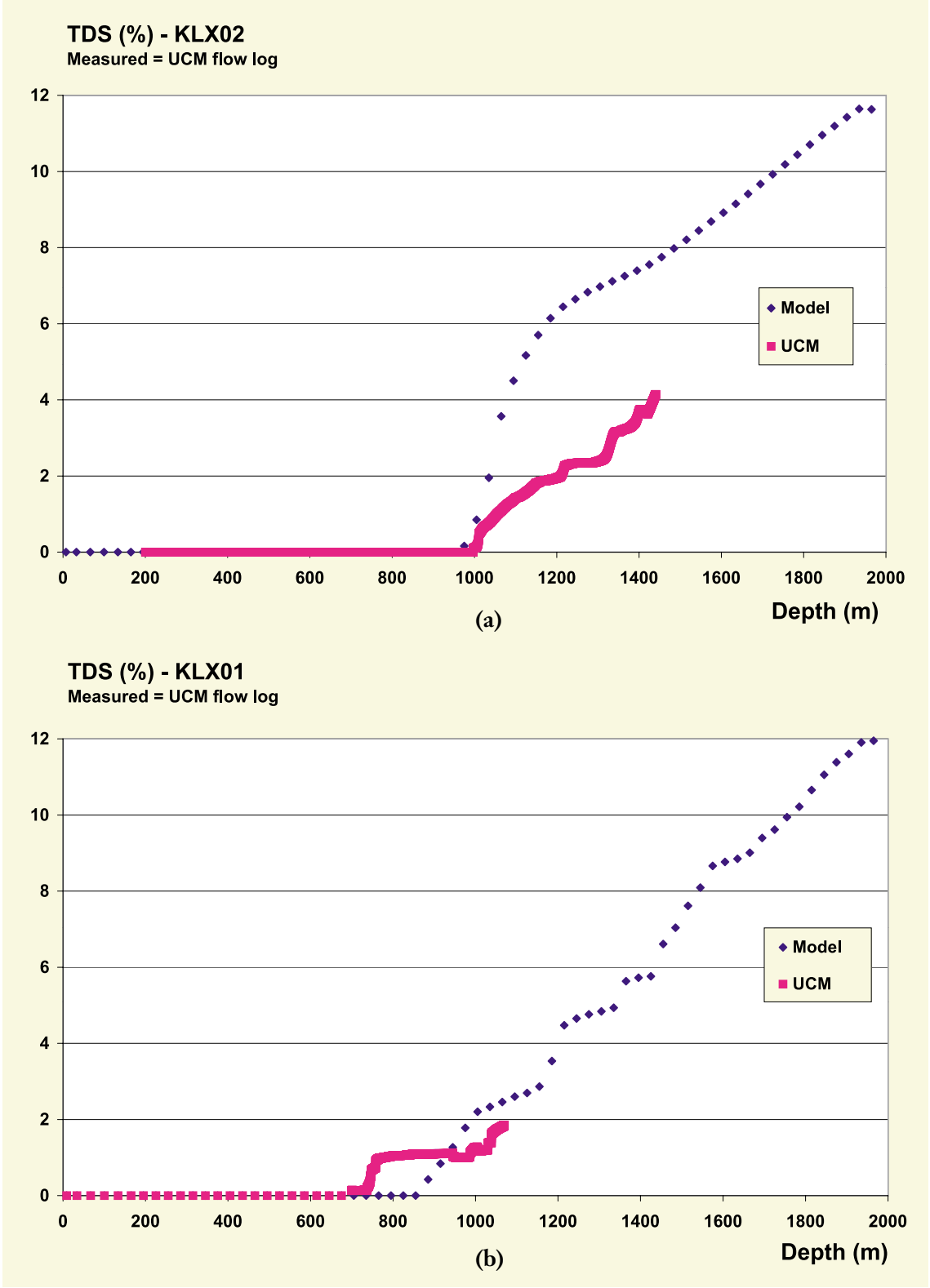

Figure 4-11. *Comparison between measured and simulated salinity profiles in the two boreholes KLX02 (a) and KLX01 (b).*

Comparison between the measured and simulated upconing effects

According to the documentation of the interference test /Follin, 1996/, the measured salinity of the abstracted water in the pumped test section in borehole KLX02 was c. 1.7% (~3 000 mS/m) at the end of the test period. The simulated salinity in the model varies along the stretch of the modelled borehole, which makes it difficult to make a direct comparison. However, prior to the interference test, the simulated salinity at 975 m was 0% and at 1 065 m c. 2.5%, see Figure 4-11 (a). At the end of the simulation of the interference test, the salinity was 0.1% at 975 m and c. 4.3% at 1 065 m. Figure 4-12 indicates that the are tiny, but noticeable, changes in the salinity field due to the simulated test pumping. The result is interesting given the fact that the flow rate of the interference test is fairly small. That is, it may of interest to look more closely at the possibility to use the salinity as a tracer during the hydraulic testing.

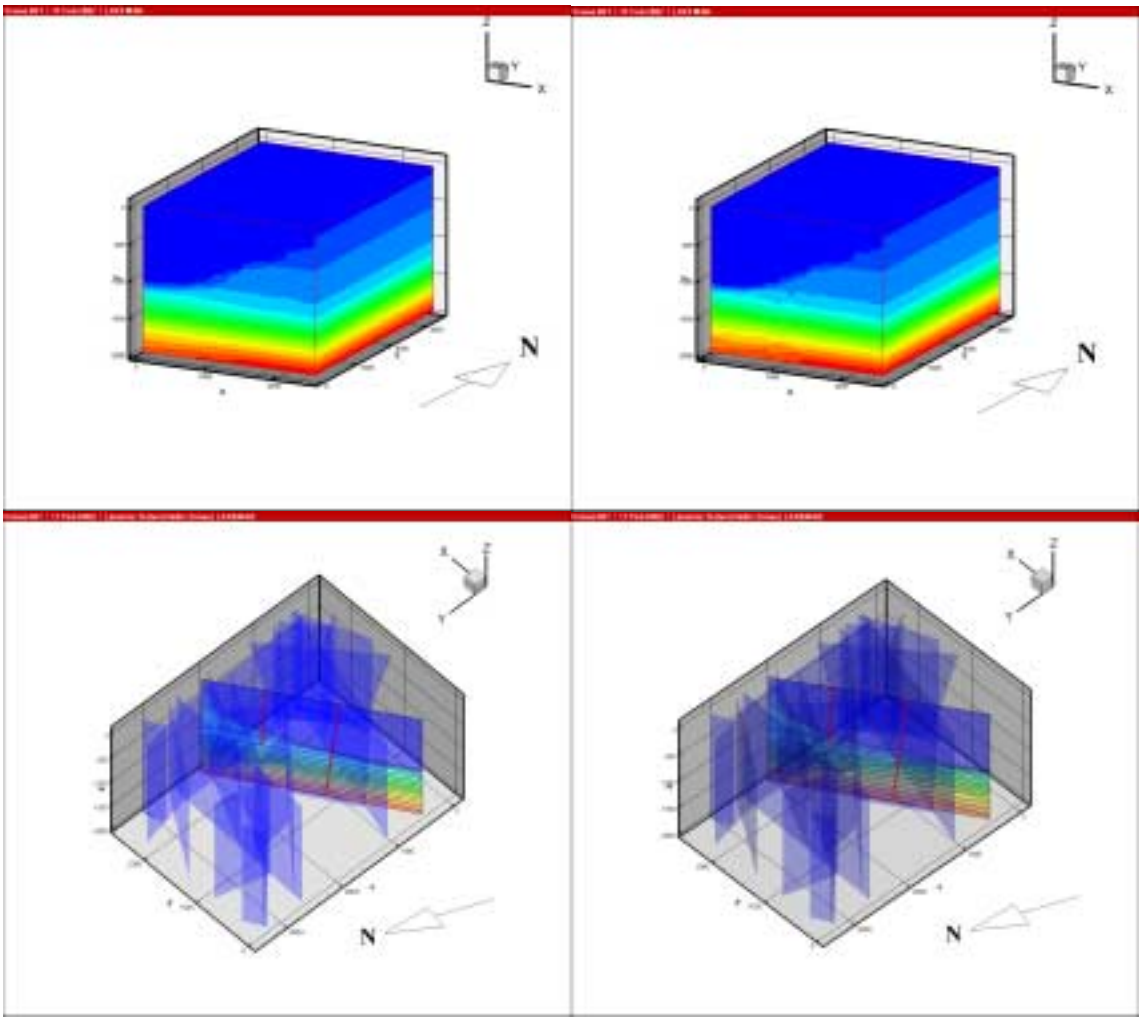

Figure 4-12. *Comparison between undisturbed (left) and disturbed (right) conditions. The test pumping causes a small, but noticeable, wiggling in the salinity field.*

5 Discussion of results and uncertainties

The work presented in this report has been carried out to reach the following objectives:

- construct a numerical flow model on a local scale, corresponding to version 1.2, for the Laxemar area,
- through numerical simulations test (as well as contribute to) the evaluation and integration of site specific information with the planned methodology,
- through numerical simulations increase the understanding of the Laxemar area and, if possible, demonstrate how a creditability of the numerical flow model can be achieved/increased, and
- document experiences and uncertainties as well as suggest potential developments of current modelling methodology.

The outcome of the work is documented in Chapters 2–4 except for the last objective, which is treated in this Chapter. It is important to note that, the present project has primarily been concerned with testing. The numerical flow model that has been constructed in support of the methodology test project should be reasonable, but it can not be regarded as a "real" version 1.2 as there are limitations both in input data and in the scope of the analysis. Conclusively, only general conclusions, at the most, can be drawn from the results presented in this report.

5.1 Size of model domain and boundary conditions

The size of the Laxemar model domain was decided by the methodology test project prior to the execution of the numerical modelling study. Subsequently, it was decided that the numerical modelling study should adopt the size of the model domain "as is" and treat the boundary conditions accordingly. To the extent possible, the results from the regional numerical flow modelling conducted by /Svensson, 1997a/ have been used as a means to evaluate the implications of the chosen size of the Laxemar model area as well as the chosen boundary conditions. Although it can be advocated that the chosen boundary conditions and the chosen state of flow (steady state) in the present study are sufficient to meet the objectives of the methodology test project, it is recognised that the issue on a whole is superficially treated. For instance, regional flow and shore level displacement are two examples of processes that probably need to be treated more thoroughly.

5.2 Salinity

The steady state simulations of saline groundwater appear to match the interface between fresh and saline groundwater in the boreholes KLX01 and KLX02. If this interpretation is correct, the current rate of the ongoing shoreline displacement process in this region of Sweden (1.5 mm per year) might be sufficiently slow in order to allow for a "Ghyben-Herzberg stabilisation" of the pressure field, at least along the stretch of the boreholes and at some distance from the sea. Since the role of a varying kinematic porosity is overruled by the assumption of steady state flow, one cannot be more conclusive on this matter. The simulations suggest, however, that it may be of interest to look more closely at the possibility to use the salinity as a tracer during the hydraulic testing.

5.3 Hydraulic conductor domain

The methodology test project group decided that the numerical modelling study should adopt the Base geological model as the one and only representation of the deterministic hydraulic conductor domain in the Laxemar area. The Alternative geological model mentioned in Chapter 3 has not been dealt with, although it is recognised that the discrimination between alternative geological models by means of exploration simulations is probably one of the more important tasks.

Alternative geological models represent another kind of uncertainty than the uncertainty that is treated in a probabilistic fashion. Alternative geological models may be regarded as provisional 'deterministic' geological models, the soundness of which can be judged through geoscientific hypothesis testing. That is, by means of qualified field investigations in combination with numerical explorations, it can be concluded which alternatives that disqualify and which that cannot be disqualified. Ideally, one would hope that there is only one remaining model at the end, which suggests that the process of confidence building has a unique solution. It should be noted, however, that hypothesis testing is a method by which we can disprove a theory, not prove. Hence, the ultimate "one and only" is a working hypothesis, which in time due will lend itself to alternative interpretations, which in turn need to be scrutinised and tested geoscientifically. Hypothesis testing is an evolving process though, with a clear objective – demonstrate creditability.

Geoscientific hypothesis testing is by and large a matter of co-interpretation of different types of geoscientific information such geological, geophysical, hydrological, hydrogeological and hydrogeochemical data. For instance, it is noted in Chapter 4 that the Alternative geological model of the Laxemar area is very interesting as compared to the Base geological model. One of the more interesting facts is that the co-interpretation of geological-geophysical data shows up to be very interesting also from a hydraulic point of view. The point made here is that the co-interpretation of the geological-geophysical data was made prior to incorporation of the hydraulic information, which definitely increases the creditability of the Alternative model.

Despite the interdisciplinary collaboration, however, there are still significant single-hole test section transmissivities in the two boreholes KLX01 and KLX02 that are not well explained by any of the two available geological models. This result suggests that there is more work needed before one can be more conclusive on how to proceed with the representation of the hydraulic conductor domain. Alternatively, the version 1.2 numerical model will have to treat high test section transmissivities in a probabilistic fashion, see Section 5.4 domain.

5.4 Hydraulic rock domain

In contrast to deterministic models, probabilistic models for the rock mass between the major fracture zones can treat field data that are highly heterogeneous, which cannot be described with creditability in a deterministic fashion. Probabilistic models invoke stochastic theory and Monte Carlo realisations as a means of handling the heterogeneity in the observations and the uncertainty about the unseen.

Monte Carlo realisations can be unconditional or conditional. Unconditional realisations honour the ensemble statistics of the available geometric and hydraulic information, but not the local information as such. The process of honouring local information, e.g. borehole data at specific locations, is called conditioning. The implications of working solely with unconditional realisations in the hydrogeological modelling of the hydraulic rock domains are judged to be important and need to be discussed and resolved.

The problem that needs to be treated is how to condition groundwater flow through a discrete fracture network. Unlike porous media, flow through fractured rocks is extremely difficult to characterise since the flow paths are both geometrically and hydraulically constrained. Secondly, the database is very limited and the observations of fracture intersections with boreholes are extremely local given the huge volume of rock that is treated. For instance, the Laxemar model domain is 17 km^3. Thirdly, the sizes of the intersecting fractures cannot be determined deterministically, unless they are very large and/or intersected by a large number of boreholes. Fourthly, there is generally a very poor correlation between the fracture frequency and the test section transmissivity, due to the fact that (*i*) some fractures have closed intersections or isolated, and (*ii*) the transmissive fractures have different apertures. For example, the cumulative flow through two parallel fractures each with a hydraulic flow aperture of e is much less than the flow through a single fracture with an aperture of $2e$ (cf. Section 2.2.3). Also, the suggested correlation between fracture size and transmissivity is tentative. The full spectrum of describing uncertainty in the rock mass would require testing other functional relationships including no correlation whatsoever.

No efforts have been made to treat the problem of conditioning in the present study due to the limitations in scope of the methodology test project. However, as a contribution to the ongoing discussion about the pros and cons of alternative methods, it is suggested here to test a variant where the unconditional Monte Carlo realisations are altered hydraulically but not geometrically at the borehole intercepts. That is, the transmissivities of the probabilistic fractures are adjusted in proportion to their proportion of the cumulative transmissivity wherever they intersect a borehole section with a given test section transmissivity, see Figure 5-1.

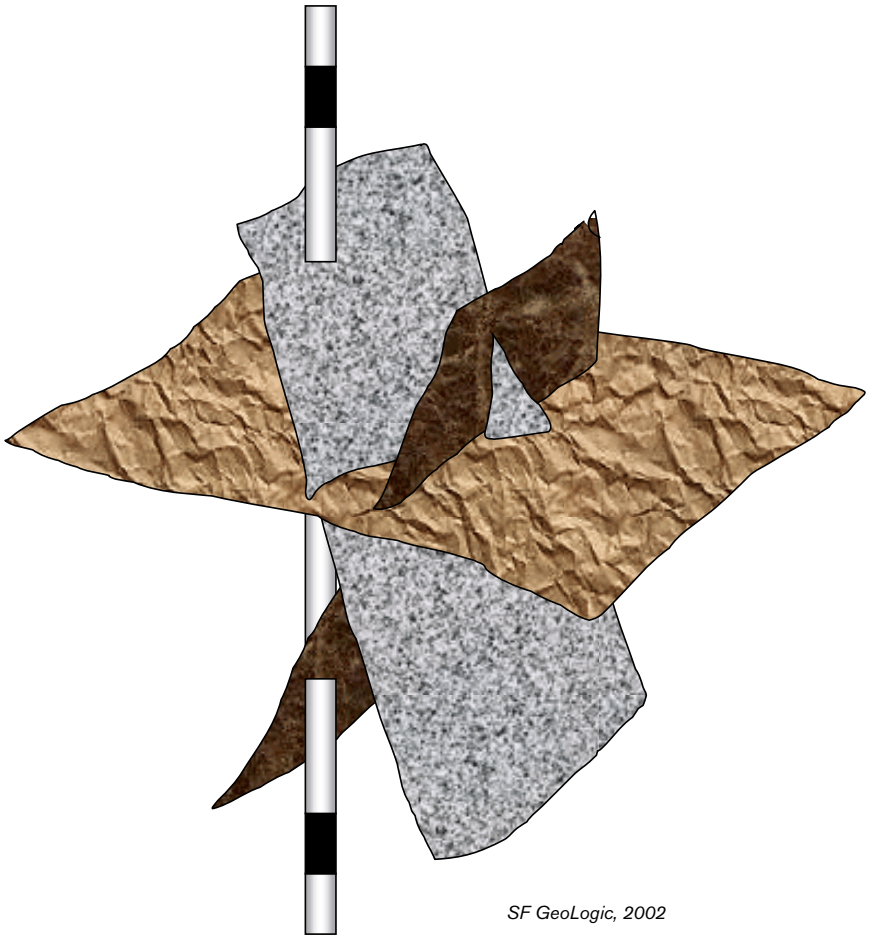

Figure 5-1. *Probabilistic fractures intersecting a bore test section.*

5.5 Hydraulic soil domain

Most groundwater models are incapable of treating surface runoff in a correct way. The intermediate version of DarcyTools is an exception in this sense. The point made here is that an appropriate treatment of the hydrogeological conditions on the top boundary is important for the creditability of the entire modelling. Questions like "How large will the radius of influence be once the construction of the deep repository has started?" require a good understanding of the conditions that govern the relation between the net precipitation and the maximum groundwater recharge. Conclusively, it is important to have a good control of surface runoff parameters such as lake elevation verges and stream flow rates, but also the thickness and conductivity of the Quaternary deposits.

The performed tuning of the hydraulic conductivity of the uppermost layers carried out in support of this project is by no means exhaustive. The major limitation is the lack of data. In order to circumvent costly and time consuming ground investigations, it is suggested to pay attention to the problem already from the onset during the site investigations. Unfortunately, the methodology test project group did not have enough time to focus on the possibilities to gather different sources of near surface information into a GIS system, and develop and interdisciplinary model for the top boundary of the Laxemar area.

5.6 Hydro-philosophy

Although DarcyTools is not perquisite for the methodology test project, the underlying hydro-philosophy of DarcyTools is inevitably an important part of the modelled system. It should be noted, however, that the hydro-philosophy of DarcyTools rests on two cornerstones, both of which are open questions. The two cornerstones are (*i*) a power law fracture size distribution L_f and (*ii*) positive correlations between the hydraulic and transport properties, e.g. T_f, b_f and e_T, and L_f, see Chapter 2. Ideally, the performed numerical simulations should have explored to what extent the two cornerstones affects the simulation results (cf. Section 5.4).

Depending on the magnitudes of the exponent and the intensity of the power law distribution, the hydraulic behaviour of a discrete system can be tuned to work more or less as a continuum. In this sense, it is noteworthy that the values used in this report are more "discrete" than the values derived by the DFN analysis in Section 3.8 of the methodology test report. From a methodological point of view, it is advocated here that it is of great interest to conduct a detailed fracture trace investigation, where the impact of the censoring effect is in focus. For the time being, the possibility for a censoring bias in the trace size analyses cannot be excluded.

6 References

Andersson J, Berglund J, Follin S, Hakami E, Halvarson J, Hermanson J, Laaksuharju M, Rhen I, Wahlgren C-H, 2002. Testing the Methodology for Site Descriptive Modelling. SKB TR-02-19, Svensk Kärnbränslehantering AB, Stockholm.

Barton C, La Pointe P R, 1995. Fractals in the Earth Sciences. Plenum Press, ISBN 0 306 44865 3.

Bear J, 1979. Hydraulics of Groundwater. McGraw-HiII, Inc. ISBN 0 070 04170 9.

de Marsily G, 1986. Quantitative Hydrogeology. Academic Press, Inc. ISBN 0 12 208915 4.

Ekman L (ed.), 2001. Project Deep Drilling KLX02, Phase 2. Methods, scope summary and results. Summary report. SKB TR-01-11, Svensk Kärnbränslehantering AB, Stockholm.

Follin S, 1993. Djupborrning KLX02 – Etapp 1, Lilla Laxemar, Oskarshamns kommun. Evaluation of the hydraulic testing of KLX02. SKB AR-94-2l, Svensk Kärnbränslehantering AB, Stockholm.

Follin S, 1996. Djupborrning KLX02 – Etapp 2, Lilla Laxemar, Oskarshamns kommun. Interpretation of the hydraulic testing of KLX02. SKB U-96-32, Svensk Kärnbränslehantering AB, Stockholm.

Follin S, Årebäck M, Axelsson C-L, Stigsson M, Jacks G, 1998. Förstudie Oskarshamn. Grundvattnets rörelse, kemi och långsiktiga förändringar. SKB R-98-55, Svensk Kärnbränslehantering AB, Stockholm.

La Pointe R, Cladouhos T, Follin S, 1999. Calculation of displacements on fractures intersecting canisters induced by earthquakes: Aberg, Beberg and Ceberg examples. SKB TR-99-03, Svensk Kärnbränslehantering AB, Stockholm.

Munier R, Hermanson J, 2001. Metodik för geometrisk modellering. Presentation och administration av platsbeskrivande modeller. SKB R-01-15, Svensk Kärnbränslehantering AB, Stockholm.

Påsse T, 1996. A mathematical model of the shore level displacement in Fennoscandia. SKB TR-96-24, Svensk Kärnbränslehantering AB, Stockholm.

Påsse T, 1997. A mathematical model of past, present and future shore level displacement in Fennoscandia. SKB TR-97-28, Svensk Kärnbränslehantering AB, Stockholm.

Rhén I, Gustafson G, Stanfors R, Wikberg P, 1997. Äspö HRL – Geoscientific evaluation 1997/5. Models based on the site characterisation 1986–1995. SKB TR-97-06, Svensk Kärnbränslehantering AB, Stockholm.

SKB, 1999. SR 97 – Post-closure safety. SKB TR-99-06, Svensk Kärnbränslehantering AB, Stockholm.

SKB, 2001. Site investigations: Charaterisation methods and general execution programme. SKB TR-01-29, Svensk Kärnbränslehantering AB, Stockholm.

Stanfors R, Erlström M, Markström I, 1997. Äspö HRL – Geoscientific evaluation 1997/1. Overview of site characterisation 1986–1995. SKB TR-97-02, Svensk Kärnbränslehantering AB, Stockholm.

Stigsson M, Outters N, Hermanson J, 2000. Prototype Repository – Hydraulic DFN model No. 2. Final Draft submitted to SKB, Svensk Kärnbränslehantering AB, Stockholm.

Svensson U, 1997a. A regional analysis of groundwater flow and salinity distribution in the Äspö area. SKB TR-97-09, Svensk Kärnbränslehantering AB, Stockholm.

Svensson U, 1997b. A site scale analysis of groundwater flow and salinity distribution in the Äspö area. SKB TR-97-17, Svensk Kärnbränslehantering AB, Stockholm.

Svensson U, 1999. Representation of fracture networks as grid cell conductivities. SKB TR-99-25, Svensk Kärnbränslehantering AB, Stockholm.

Svensson U, 2001. Groundwater flow, pressure and salinity distributions around the Prototype Repository. SKB IPR-01-40, Svensk Kärnbränslehantering AB, Stockholm.

Svensson U, Kuylenstierna H-O, Ferry M, 2002. DarcyTools. Concepts, methods, equations and tests. Version 1.0. Draft report submitted to SKB March 2002, Svensk Kärnbränslehantering AB, Stockholm.

Turcotte D L, 1992. Fractals and chaos in geology and geophysics. Cambridge University Press, ISBN 0 521 41270 6.

Vicsek T, 1989. Fractal growth phenomena. World Scientific Publishing Ca. Pte. Ltd, ISBN 9971 50 442 X.

Voss C, 1984. SUTRA – A finite-element simulation model for saturated-unsaturated fluid den sit y- dependent groundwater flow with energy transport or chemically reactive single-species solute transport. Water Resources Investigation Report 84-4369, U.S. Geological Survey, Reston.

Walker D, Gylling B, 1998. Site-scale groundwater flow modelling of Aberg. SKB TR-98-23, Svensk Kärnbränslehantering AB, Stockholm.

Westman P, Wastegård S, Schoning K, Gustafsson B, Omstedt A, 1999. Salinity change in the Baltic Sea during the last 8,500 years: evidence, causes and models. SKB TR-99-38, Svensk Kärnbränslehantering AB, Stockholm.